

Foraminifera of the Faneromeni section (Crete, Greece) reflect the palaeoenvironmental development towards the Messinian salinity crisis

Jing Lyu^{a,*}, Tanja J. Kouwenhoven^a, Roberta Calieri^b, Lucas J. Lourens^a

^a Department of Earth Sciences, Utrecht University, Princetonlaan 8a, 3584, CB, Utrecht, the Netherlands

^b ENI Spa, Piazza Enzo Vanoni, 1 / Via Emilia, 1, San Donato Milanese (MI), Italy

ARTICLE INFO

Keywords:

Benthic and planktic foraminifera
Palaeoecology
Eastern Mediterranean
Messinian restriction
Precessional cyclicity

ABSTRACT

A severe phase of disturbance around 7.17 Ma initiated an ongoing development towards the Messinian salinity crisis (MSC) of the Mediterranean. We present foraminiferal data from the Faneromeni section on Crete to understand how the astronomical cyclicity and the restriction phase starting at 7.17 Ma were reflected in a succession that was deposited on the continental shelf and characterized by a precession-dominated alternation of organic-enriched grey marls and sapropels and light-coloured homogeneous marls. Benthic and planktic abundance data show that the foraminifera are closely associated with precessional cyclicity. Similar as in other Mediterranean sections, the 7.17 Ma shift in benthic assemblages is sedimentologically expressed by the occurrence of the first distinct sapropel (Faneromeni cycle F18). At this level, throughout the Mediterranean a group of open marine benthic species intolerant to oxygen stress abruptly decreased in abundance with several species disappearing at or shortly after 7.17 Ma. These species were replaced by species indicating increasing stress, implying decreasing oxygen content of the bottom waters after 7.17 Ma. The data further suggests that sapropelic sediments dominated by *Bolivina dilatata/spatulata* were deposited under hypoxic conditions, rather than under continuous organic flux. Our data reflects a second step in the restriction of the Mediterranean between 6.8 and 6.7 Ma, indicated by decreasing benthic diversity and increasing abundances of planktic and benthic taxa considered tolerant of hypersalinity. An increase in water salinity has been suggested before, and if true, appears to have affected the bottom waters and the surface waters around the same time.

1. Introduction

The Messinian salinity crisis of the Mediterranean Sea (MSC) is widely regarded as one of the most dramatic episodes of oceanic change of the past 20 million years, leading to the most recent salt giant in geological history (Hsü et al., 1973; Roveri et al., 2014; Flecker et al., 2015). The start (5.971 Ma: Manzi et al., 2013) and end of the MSC (5.33 Ma: Van Couvering et al., 2000) were earlier found to occur synchronously across the Mediterranean (e.g., Hilgen et al., 2007). Recently however, a synchronous start of the MSC has been challenged again. Manzi et al. (2021), based on material obtained from commercial drilling in the Levantine Basin, proposed that although the onset of the MSC was synchronous, the start of evaporite deposition was diachronous. A recent study by Zachariasse and Lourens (2021) on land-based sections throughout the Mediterranean resulted in an updated age of the MSC onset on Sicily and Gavdos (south of Crete) to 6.00 Ma, implying an age

offset between eastern and western Mediterranean basins of some 30 kyrs.

Previous research showed that the ongoing development towards the MSC started around 7.17 Ma, more than a million years before the first Messinian evaporites were deposited (e.g., Santarelli et al., 1998; Seidenkrantz et al., 2000; Kouwenhoven et al., 2003), and was approximately synchronous with uplift in the Betic and Rifian Corridors in southern Spain, respectively northern Morocco (~7.2 Ma: Krijgsman et al., 1999; ~7.17 Ma: Bulian et al., 2021), the known late Miocene gateways connecting the Mediterranean with the Atlantic Ocean and part of the Gibraltar Arc (e.g., Roveri et al., 2014; Flecker et al., 2015 and references therein). The timing of closure of the Betic and Rifian Corridors was recently better constrained (Martín et al., 2014; Capella et al., 2017; Tulbure et al., 2017; Capella et al., 2018; Van der Schree et al., 2018) and probably predated the start of the salinity crisis, but there is no conclusive evidence of which Mediterranean-Atlantic

* Corresponding author.

E-mail address: jlyu@marum.de (J. Lyu).

¹ Presently at: MARUM, University of Bremen, Leobener Str. 8, 28,359, Bremen, Germany

gateway contributed the large quantity of salt into the Mediterranean Sea during the MSC. Capella et al. (2018), Capella et al. (2019) and Krijgsman et al. (2018) recently proposed that the Gibraltar Corridor might have been the sole connection with the Atlantic Ocean remaining open during most of the MSC.

Sedimentological, geochemical, floral and faunal proxy data and modelling studies have been applied to constrain the connection history of the Mediterranean with the Atlantic (overviews in Roveri et al., 2014; Flecker et al., 2015). Planktic flora and fauna were sensitive both to astronomical cyclicity and to connection dynamics (e.g., Sprovieri et al., 1996; Santarelli et al., 1998; Pérez-Folgado et al., 2003; Sierro et al., 2003; Flores et al., 2005; Zachariasse et al., 2021). Similarly, benthic foraminiferal distributions were influenced by astronomical forcing, but in addition reveal a major Mediterranean-wide turnover of benthic foraminifera, at multiple locations from Spain to Cyprus, around 7.17 Ma (Kouwenhoven et al., 2003; Corb   et al., 2020; Bulian et al., 2022). This event coincides with the deposition of a distinct sapropel, which has been tuned to the first amplified precession minimum at 7.17 Ma succeeding the 400-kyr eccentricity minimum around 7.25 Ma (Hilgen et al., 1995). Benthic foraminiferal assemblages indicating stressed bottom-water environments (among others containing bolivinids and buliminids) were abundant after 7.17 Ma, whereas the taxa intolerant to stressed bottom-water environments, such as *Cibicides wuellerstorfi*, *Cibicoides italicus* and *Siphonina reticulata* disappeared (e.g., Seidenkrantz et al., 2000; Blanc-Valleron et al., 2002; Kouwenhoven et al., 2003; Kouwenhoven et al., 2006; Violanti et al., 2007; P  rez-Asensio et al., 2012; P  rez-Asensio et al., 2014).

The effect of the 7.17 Ma event on the benthic foraminiferal assemblages of the Faneromeni section (Crete, Greece, eastern Mediterranean; Fig. 1) appeared to be minor (Kouwenhoven et al., 2003), and certainly less severe than in the bathyal sections of Monte del Casino (Apennine foothills), Gibliscemi (Sicily) and Metochia (Gavdos), where the event was well expressed in the homogenous marls (Kouwenhoven et al., 2003). To assess whether the event at 7.17 Ma is better expressed in the Faneromeni section when the grey marls and sapropels are taken into consideration, a high-resolution study of benthic and planktic foraminifera of the Faneromeni section has been conducted. In this study, new benthic foraminiferal assemblage data derived from grey marls and sapropels were added to the data of the light-coloured marls studied previously (Kouwenhoven et al., 2003) and combined with selected data of planktic foraminifera (Calieri, 1996). Effects of astronomical cyclicity on the Messinian surface- and bottom-water palaeoenvironments are further explored by evaluating the

palaeoenvironmental signals reflected by the benthic and planktic foraminiferal assemblages. This way, a more comprehensive interpretation is pursued of the palaeoenvironmental development at Faneromeni during the latest Tortonian and the early part of the Messinian preceding the MSC (7.62–6.68 Ma), with emphasis on the 7.17 Ma event.

2. Background

2.1. Geological setting

The island of Crete has moved southward to its present position during opening of the Aegean extensional forearc, which is part of the Aegean continental extensional province. Opening of the forearc was related to south-westward retreat (slab roll-back) of the African promontory subducting beneath Eurasia, as a consequence of Africa-Eurasia convergence closing the Tethyan seaway (e.g., Jolivet et al., 2006; Van Hinsbergen and Meulenkamp, 2006 and references therein). Southward migration and subsidence of Crete was followed by uplift during the Pliocene (Zachariasse et al., 2008 and references therein), exposing a mosaic of late Miocene and younger marine and fluvio-lacustrine sequences on top of metamorphic basement. Work on the complicated structural development of Crete is still ongoing (e.g., Zachariasse et al., 2011 and references therein; Martha et al., 2018).

The position of Crete is relatively close to the Aegean Sea where during the late Miocene, in the northern section, a land-locked basin existed with shallow connections to the Mediterranean Sea and Paratethys (Krijgsman et al., 2020). Marine incursions reached the north Aegean during the Messinian and a semi-isolated Egemar Sea developed between 6.9 and 6.1 Ma, when the Mediterranean Sea and Paratethys became intermittently connected. Despite its location, relatively close to the Dodekanisos Seaway: the projected southern connection between Egemar and the Mediterranean Sea, Crete is, and was during the Messinian, part of the Mediterranean domain (Krijgsman et al., 2020 and references therein).

2.2. The Faneromeni section

The Faneromeni section is located on the north-east coast of Crete (Fig. 1a, b) and covers the latest Tortonian to early Messinian in a near-continuous sediment sequence with a slumped level at 53 m (Fig. 2, 3). The section contains cyclic alternations of light-coloured, sometimes sandy, blueish or beige (hereafter ‘light’) carbonate-rich marls, and darker, more weathered and more clayey grey-green-blue coloured

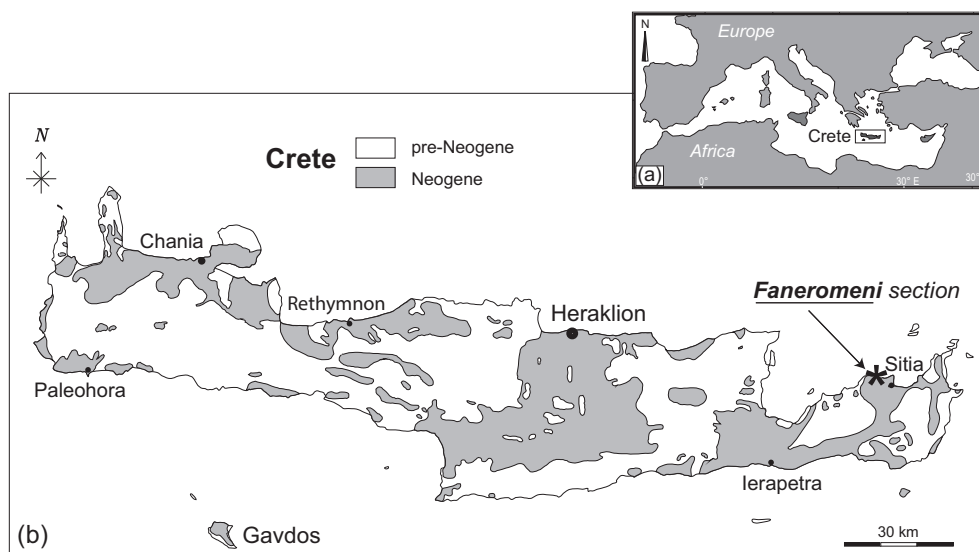


Fig. 1. a: Map of the Mediterranean area with location of Crete; b: Map of Crete with location of the Faneromeni section. Modified from Krijgsman et al., 1994.

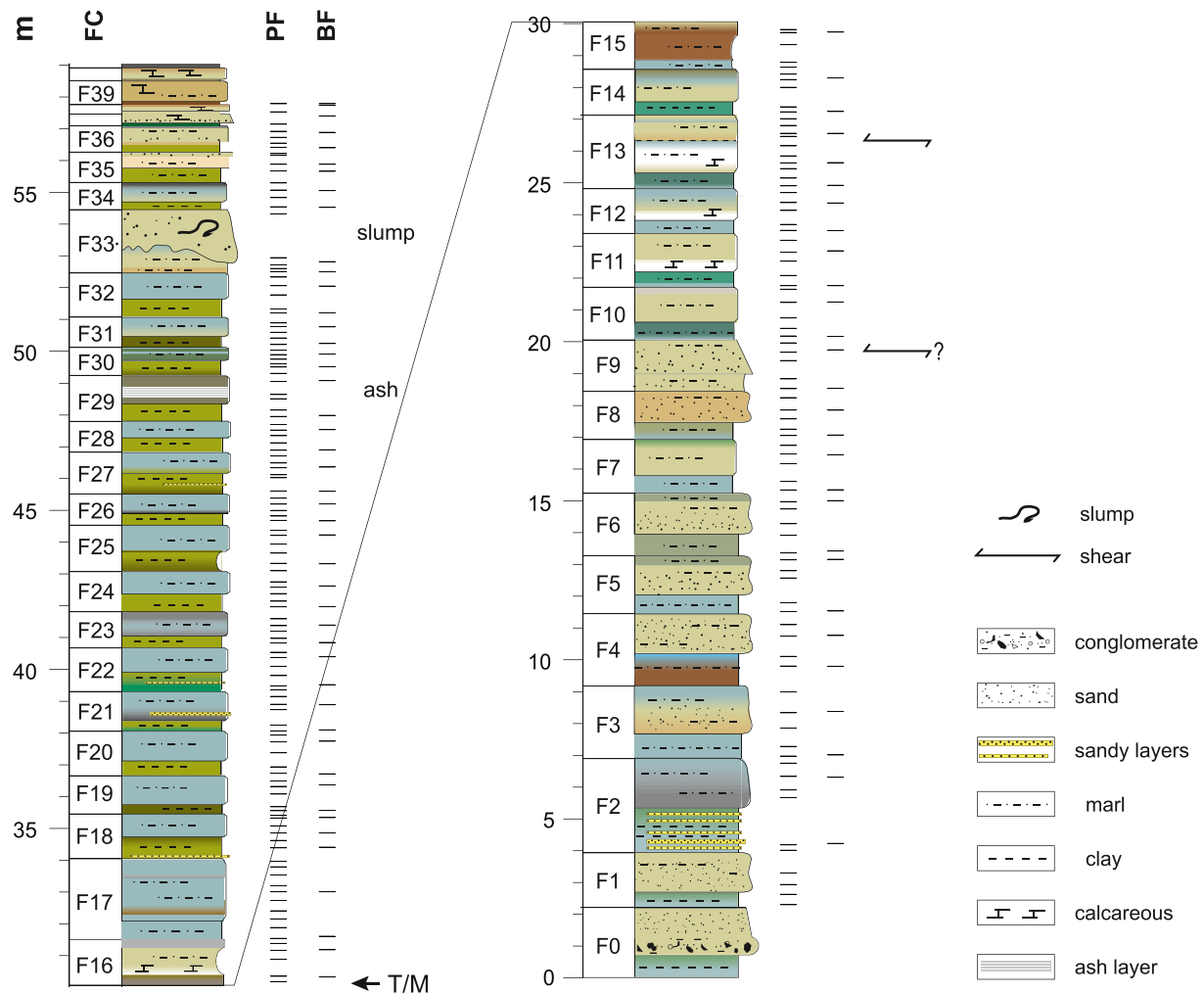


Fig. 2. Stratigraphic log of the Faneromeni section. Abbreviations: **m** = stratigraphic level in metres; **FC** = Faneromeni cycle number; **PF** = samples studied for planktic foraminifera; **BF** = samples studied for benthic foraminifera; **T/M** = Tortonian-Messinian boundary (7.246 Ma: Hilgen et al., 2000; Hilgen et al., 2012).

(hereafter 'grey') carbonate-poor marls in the lower part until cycle F18, while green-brownish coloured sapropelic layers (hereafter 'sapropelic layers') are dominantly interlayered with the light marls from cycle F18 upwards. Grey marls and particularly sapropels occur in large-scale clusters that contain 3 or 4 small-scale clusters (containing 3 or 4 sapropels) and are separated from adjacent clusters by generally thicker and more indurated light-coloured marly intervals. In the top of the section, around 57 m, the marls become more calcareous and brownish clay layers develop instead of sapropels.

The age of the Faneromeni section has been constrained by biostratigraphy (Langereis et al., 1984; Calieri, 1996; Negri and Villa, 2000), magnetostratigraphy (Krijgsman et al., 1994) and cyclostratigraphy (Hilgen et al., 1995; Krijgsman et al., 1995). The sedimentary cycles in the Faneromeni section can be interpreted with the Earth's orbital cycles of precession, obliquity (tilt) and eccentricity (Hilgen et al., 1995). Individual sapropels are related to precession minima (insolation maxima), while sapropel clusters are related to eccentricity maxima. Alternation of thick/thin or present/absent sapropels reflects interference between precession and obliquity (Hilgen et al., 1995). Hilgen et al. (1995) calibrated the sedimentary cycles of the sections directly to the 65° N summer insolation curve of astronomical solution La90 with present-day values for the dynamical ellipticity of the Earth and the tidal dissipation by the moon (La90: Laskar, 1990; Laskar et al., 1993), which provided astronomical ages for all sedimentary cycles (Appendix A of Hilgen et al., 1995; Fig. 2, 3). Using among others the Faneromeni data,

Krijgsman et al. (1995) refined the age of the Tortonian-Messinian boundary, which was further constrained by Hilgen et al., 2000 and Hilgen et al., 2012. The time scale is consistent with $^{40}\text{Ar}/^{39}\text{Ar}$ ages of volcanic beds in, among others, Faneromeni (Kuiper et al., 2004) and with the number of sedimentary cycles in the younger, partly evaporitic part of the Mediterranean Messinian (Hilgen et al., 1995). In this study the age model of Hilgen et al. (1995) and Krijgsman et al. (1995) is adhered to, facilitating correlation with publications on other Mediterranean sites, despite recent (partial) modifications of the age model for the purpose of calibration of the Fish Canyon sanidine (Rivera et al., 2011; Phillips et al., 2017).

2.3. Previous palaeoenvironmental investigations

Previous work on microfossils in the Faneromeni section includes among others palaeoecology based on calcareous plankton and benthos (Negri and Villa, 2000; Kouwenhoven et al., 2003), and dinoflagellate cysts (Santarelli et al., 1998), who also explored orbital signatures in their data. An integrated, detailed geochemical and micropalaeontological study of three sapropels of the Faneromeni section was performed by Nijenhuis et al. (1996), who concluded that increased seasonality and higher export production were associated with the deposition of sapropels. Moissette et al. (2018) performed a sedimentological and floral/faunal study on three Cretan sections, among which the Faneromeni section, and found dysoxic episodes during the

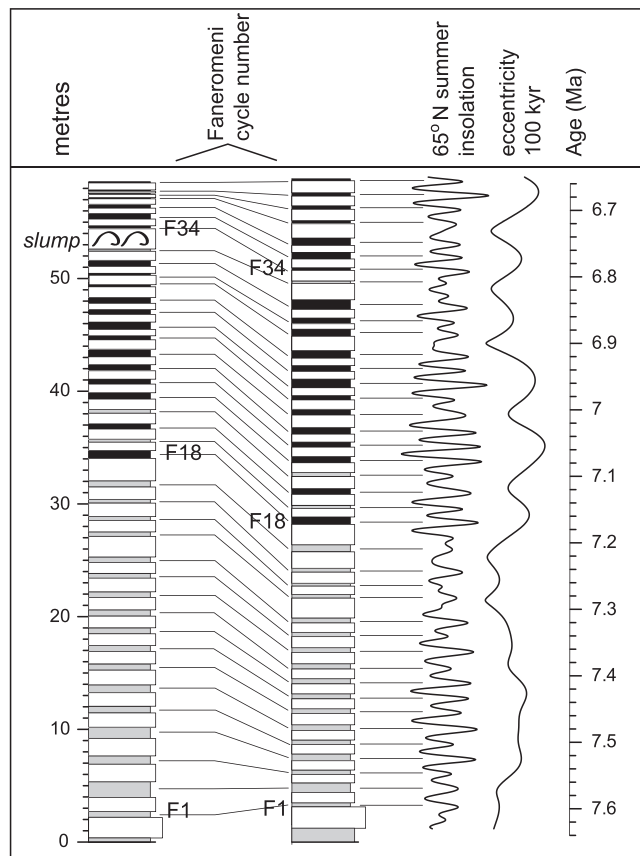


Fig. 3. Schematic lithology of the Faneromeni section in the depth and time domain. After Hilgen et al., 1995.

White = homogeneous marl; grey = grey marl; black = sapropelic sediment.

Messinian together with a shallowing-upward trend. Kontakiotis et al. (2019) set out to quantify temperature and salinity changes in the period preceding the MSC together with input and preservation of organic matter. The stable carbon isotope records in Kontakiotis et al. (2019) reflect the shift to lighter values starting at 7.17 Ma that was earlier found in other Mediterranean sections (Hodell et al., 1994; Hodell et al., 2001; Sprovieri et al., 1996; Seidenkrantz et al., 2000; Kouwenhoven et al., 2003) and was found to be time-equivalent with a negative carbon isotope ($\delta^{13}\text{C}$) shift of dissolved inorganic carbon (DIC) during the late Miocene in the world ocean (e.g., Keigwin and Shackleton, 1980). This $\delta^{13}\text{C}$ excursion, the late Miocene carbon isotope shift (LMCIS) occurred during a period of high marine biological productivity (Farrell et al., 1995; Holbourn et al., 2018 and references therein) and is of larger amplitude in the Mediterranean (Bulian et al., 2022). It was associated with a global cooling estimated at 6 °C (Herbert et al., 2016; Holbourn et al., 2018). In the Mediterranean, cooling was recently estimated to be in the order of ~9–10 °C in northern Italy (Monte dei Corvi) (Tzanova et al., 2015) and ~ 10 °C in the eastern Mediterranean (Faneromeni section) (Kontakiotis et al., 2019). The LMCIS event is explained by enhanced organic carbon input from terrestrial sources to the marine environment (Shackleton, 1977; Vincent et al., 1980) and shifts in the vegetation type (e.g., Cerling et al., 1997). A younger shift to heavier $\delta^{18}\text{O}$ at 6.74 ± 0.04 Ma on central Crete and the nearby island of Gavdos (Zachariasse et al., 2021; Zachariasse and Lourens, 2021) was explained by a rise in salinity.

3. Materials and methods

3.1. Sampling and sample preparation

Samples from the light marls, grey marls and sapropels of the Faneromeni section were collected by coring with a water-cooled electrical drill with sample spacing between 5 and 45 cm. The samples were washed with tap water over sieves of mesh sizes 63 μm , 125 μm and 595 μm . Splits in the size fraction 125–595- μm were obtained with a micro-splitter and then hand-picked with a water colour brush under a dissection microscope. The specimens were collected in micro-palaeontology slides, sorted, identified and counted. The procedure was standardised for planktic and benthic foraminifera.

Between 245 and 588 planktic specimens (mean: 350) in 194 samples of all lithologies: the homogeneous (light-coloured) marls, the grey and the sapropelic layers, were counted by R.C. in 1996 at the University of Bologna. Between 123 and 588 specimens (mean: 240) in 40 samples from the homogeneous marls were counted by T.K. in 1998 at Utrecht University. Newly collected by J.L. in 2020 at Utrecht University were between 140 and 576 (mean: 254) specimens of benthic foraminifera in 34 samples from the grey and sapropelic layers. The new benthic foraminifera counts from grey marls and sapropels of the Faneromeni section, together with the pre-existing data from the light marls, add up to approximately two samples per precessional cycle and 74 samples in total analysed for benthic foraminifera (Appendix B). These 74 benthic foraminifera samples were evaluated for this study and combined with a re-evaluation of the planktic foraminifera data.

3.2. Foraminiferal data analysis

Palaeoenvironments have been reconstructed using standard methods in foraminiferal palaeoecology, assessing shifts in foraminiferal assemblages. Preservation of the foraminifera was variable, between fair (lower part of the sequence) and poor (towards the top). Especially above 40 m (after ~7 Ma) the foraminifera have a quite heavily recrystallised aspect.

Because for a quantitative analysis the taxonomic concepts need to be applicable under sub-optimal conditions, supra-specific groups were used both for planktic and benthic foraminifera. The benthic morphotypes *Bolivina plicatella* and *B. pseudoplicata* were counted as *B. plicatella*, since discrimination between the two species was difficult, and moreover appears to be mainly based on the geological period in which they are found (Verhallen, 1991, p.116). Counts of *Bulimina striata* var. *mexicana* were included in *B. striata*. *Bolivina dilatata* and *B. spathulata* were counted together as *B. dilatata/spathulata*, since intermediate forms occur in the samples and their ecological signals are similar. We follow Verhallen (1991, p.117) in considering the different morphotypes as a morphocline. The *Elphidium* species were grouped for multivariate analysis because preservation was sub-optimal in the upper part of the section and detailed discrimination between species was often not feasible. Similarly, several planktic taxa used for palaeoecology were grouped. The sinistral and dextral forms of *Globorotalia conomiozea*, *G. scitula* and *Neoglobobulimina acostaensis* were taken together. *Globorotalia scitula* comprises the unkeeled globorotaliids and includes *G. prae-margaritae* and *G. nicolae*. *Orbulina* spp. includes *O. suturalis*, *O. bilobata* and *O. universa*. Also in the *Globigerinoides* spp. some species were summed; in this group *Globigerinoides obliquus obliquus* and *G. obliquus extremus* were counted together. *Globigerina bulloides* and *G. falconensis* were counted separately, although they are often grouped for palaeoecological reconstructions (e.g., Antonarakou et al., 2007). However, especially *G. bulloides* has been related to upwelling in literature (e.g., Conan and Brummer, 2000; Darling et al., 2017; Mallo et al., 2017; Wilson and Hayek, 2019).

From the raw counts the relative frequencies of planktic and benthic foraminifera, and the Shannon & Wiener index or H (for diversity) were calculated. Dry weights were used to calculate the numbers of planktic

specimens per gram of dry sediment (PF/g). For benthic foraminifera, the benthic numbers per gram of sediment (BF/g) were used to calculate benthic foraminiferal accumulation rates (BFAR).

The Shannon-Wiener diversity Index H (Hixon and Brostoff, 1983) is calculated as follows:

$$H = - \sum_{i=1}^n p_i \ln p_i,$$

where p_i is the relative frequency of the i^{th} species.

The ratio between planktic and benthic foraminifera was calculated and expressed as

$$\%P = \left(\frac{P}{P+B} \right) * 100,$$

where P and B represent counts of planktic and benthic foraminifera.

Information from literature on depth distributions of benthic foraminifera was used to further constrain palaeodepths. The percentage of calcareous shallow-water benthic taxa with a potentially epiphytic life mode (living on or near plants, within the photic zone) was calculated. These taxa include, among others, *Asterigerina planorbis*, *Discorbinella bertheloti* and other discorbids, *Bolivina plicatella*, and several *Elphidium* species (e.g., Langer, 1993; Semeniuk, 2000; Semeniuk, 2001; Moissette et al., 2007).

The planktic foraminifera were used to estimate sea-surface temperatures (SST) by calculating the ratio between warm-water species (*Globigerinoides* spp., *Globigerinella siphonifera*, *Globorotalia menardii*), and cold-water species (*G. bulloides*, *G. falconensis*, *G. scitula* and *Turborotalita quinqueloba*). In addition, the ratio between warm-oligotrophic (WO) and cold-eutrophic (CE) taxa was calculated following Sierro et al. (2003):

$$WOCE = WO / (WO + CE)$$

Warm oligotrophic taxa include *Globigerinoides obliquus*, *G. sacculifer* (syn. *Trilobatus sacculifer*), *Globigerina apertura* and *O. universa*. Cold eutrophic taxa include *G. bulloides*, *Globigerinita glutinata*, *Turborotalita quinqueloba* and the neogloboquadrinids (here mainly *Neogloboquadrina acostaensis*). This ratio was found to vary on a precessional scale during the Messinian (e.g., Pérez-Folgado et al., 2003; Sierro et al., 2003).

Data analysis included multivariate analysis, using the PAST palaeontological statistical software (Hammer et al., 2001) and was applied to relative frequency data of benthic foraminifera. Taxa with abundances below 5% in any sample were removed before the analysis to retain a robust signal of the benthic foraminiferal assemblages. This way single and scattered species occurrences were also removed. An R-mode cluster analysis (UPGMA, correlation) was performed to group the species with similar distribution patterns, and comparable ecological requirements. The same data set was introduced into Principal components analysis (PCA) to visualize important trends in the benthic foraminiferal assemblages. The first three axes of the PCA were considered, the fourth and further axes explaining only minor variance.

4. Results

4.1. Benthic foraminifera

The benthic data set contains 121 taxa (species, genera, and species groups; Appendix B). Common taxa used for palaeoecological interpretations are shown in Fig. 4. Some species, such as *Bolivina plicatella*, *Elphidium* spp. and the group of species with an epiphytic lifestyle occur mainly in the light marls, whereas others, such as *Bolivina dilatata/spatulata* and the *Uvigerina* species mainly or exclusively occur in the grey marls and the sapropelic layers. The maximum abundances of

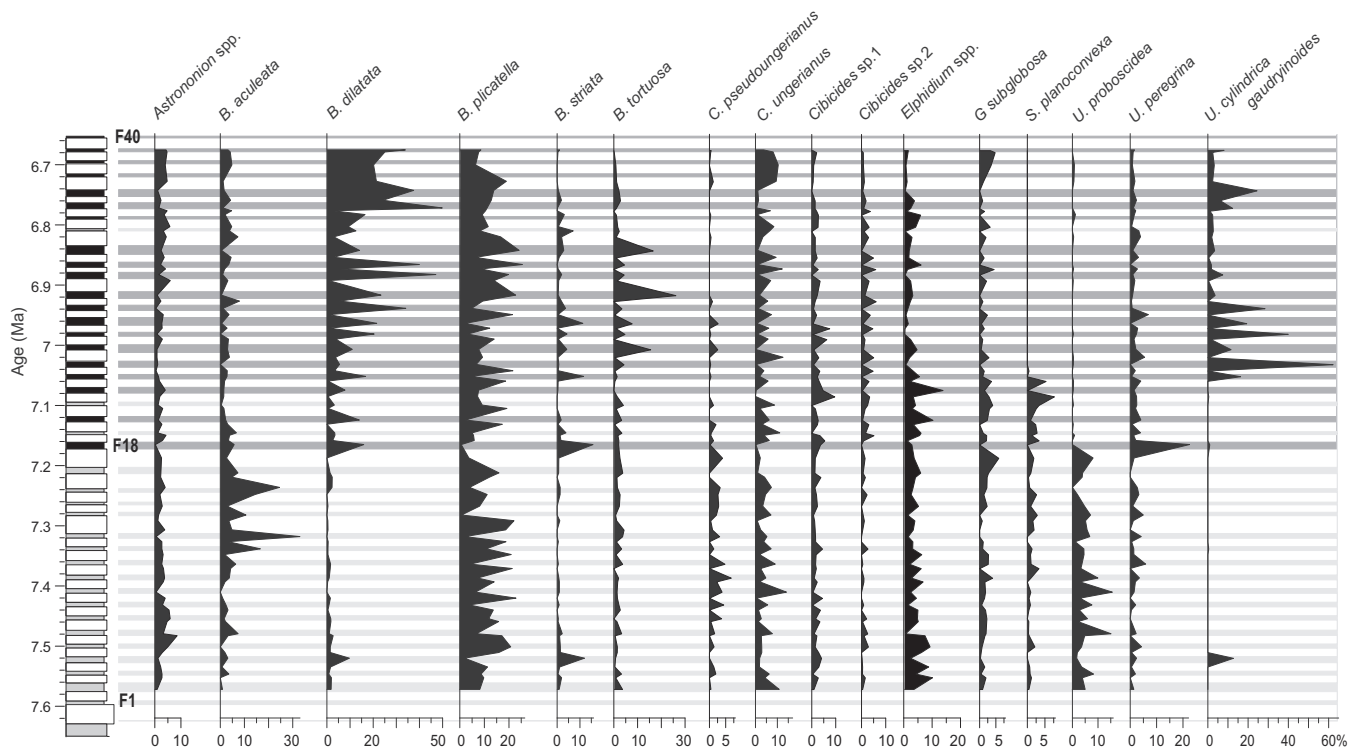


Fig. 4. Relative abundances of common benthic foraminifera in the Faneromeni section, plotted against age and schematic lithology. The lighter grey horizontal bands correspond to grey marls, the darker grey bands correspond to sapropelic layers and the white bands correspond to the light marls. The highest abundances of *Bulimina aculeata*, *Cibicides ungerianus* and *Uvigerina peregrina* shift from the grey marls below cycle F18, to the light marls above cycle F18. *Bulimina plicatella* and the *Elphidium* spp. consistently show higher abundances in the light marls. *Bolivina dilatata/spatulata* and *Uvigerina cylindrica gaudryinoides* show highest occurrences in the sapropelic layers.

Bulimina aculeata and *Cibicides ungerianus* shift from the grey marls to the light marls above cycle F18 (7.17 Ma). Bathyal species are not very abundant in the lower part of the section and even less so above cycle F18. The relative frequencies of *Uvigerina proboscidea* and *Cibicidoides kullenbergi* decrease sharply in the sapropel of cycle F18 and *Cibicidoides bradyi* and *Siphonina reticulata* disappear (Fig. 5). *Bulimina striata* and *B. aculeata* decrease in abundance after 7.17 Ma (cycle F18). Above cycle F18 the relative frequencies of *Bolivina dilatata/spathulata*, *B. tortuosa* and *Uvigerina cylindrica gaudryinoides* increase; these species, dominating the assemblages after 7.17 Ma, show temporary peaks in abundance (Fig. 4). At ~7.03 Ma a 60% peak of *Uvigerina cylindrica gaudryinoides* occurs, after which the abundance of this species gradually decreases, while *B. dilatata/spathulata* shows increasing dominance. The relative frequencies of *B. plicatella*, *Cibicides ungerianus* and *Uvigerina peregrina* remain relatively stable through time with the exception of a prominent 20% peak abundance of *U. peregrina* at 7.17 Ma. In general, the light marls are characterized by epiphytic and epifaunal to shallow infaunal species. The ratio between epifaunal and infaunal species is higher in the light marls throughout the section, whereas infaunal species dominantly occur in the grey marls and the sapropelic layers. Species tolerant to stressed bottom-water environments, such as low-oxygen conditions, reach abundances of >60% after ~7 Ma.

The sedimentation rate is decreasing upward from ~12 cm/kyr to less than 4 cm/kyr, with a maximum in cycle 33 associated with a

slumped level (Fig. 6). The accumulation rates of benthic foraminifera (BFAR in Fig. 6) are consistently higher in the light marls (Fig. 5). Except for the top of the section there is no trend towards lower mean BFAR values (~800 tests/g), despite the decreasing sedimentation rate. Below cycle F18 the pattern is regular, and it becomes more irregular after cycle F18. The ratio between planktic and benthic foraminifera (expressed as %P) fluctuates strongly (range 31.6–85.8%) over the different lithologies and is higher in the grey marls and the sapropels, the difference amounting to 40%. Especially before cycle F22 (~7.07 Ma) the pattern of %P varies very regularly on a precessional scale.

Benthic foraminiferal diversity (Shannon-Wiener index, H) fluctuates on a narrow scale between 3 and 3.5 below cycle F18 and shows maxima in the grey, as well as in the light marls. The diversity shows a highly fluctuating trend after 7.17 Ma, ranging between 2 and 3.5, reflecting a consistently higher diversity in the light marls, and lower diversity in sapropels and grey marls. The lowest value (1.97) of the H is associated with a 60% spike of *U. cylindrica gaudryinoides* at ~7.03 Ma (Fig. 4). The relative abundance of benthic taxa with a potentially epiphytic life mode is, with a mean of ~35%, higher in the light-coloured marls than in the grey and sapropelic layers (mean ~15%), with the exception of cycles F29-F33; this pattern is most regular before cycle F18.

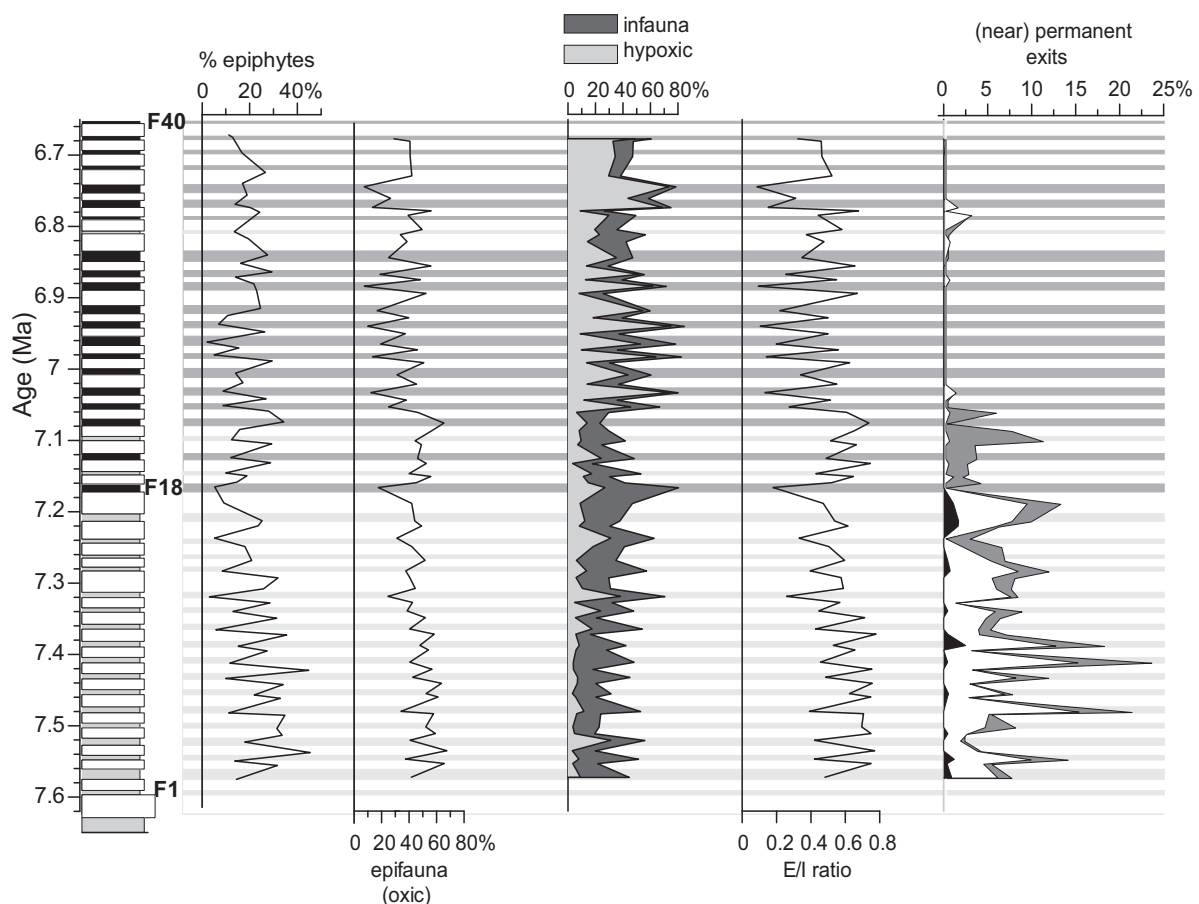


Fig. 5. Benthic foraminifera grouped according to environmental preferences. From left to right: the percentage of species that potentially live in an epiphytic habitat, including *Asterigerina planorbis*, *Bolivina plicatella*, *Cibicides lobatulus*, discorbids, *Hanzawaia boueana*, *Planorbina mediterranea* and *Rosalina* spp.; the species living in an epifaunal habitat (i.e. on, or very shallow in the top sediment layer and dependent on oxygen); the shallow and deep infaunal species, with in dark grey the shallow and deep infaunal species and in light grey the species tolerating at least temporarily moderate to severe hypoxia (among others *Uvigerina cylindrica gaudryinoides*, *Bolivina dilatata/spathulata* Group). The E/I ratio is the ratio between the epifaunal (not the epiphytic) and infaunal taxa. The panel to the right shows the bathyal species which are present in low numbers before cycle F18, and decrease in abundance at or above cycle F18: in black *Siphonina reticulata*, which disappears at this level throughout the Mediterranean, in white *Uvigerina proboscidea*, in grey the summed abundances of *Cibicidoides bradyi*, *C. kullenbergi* and *Siphonina planoconvexa* (considered a shallower living and more tolerant variety of *S. reticulata*).

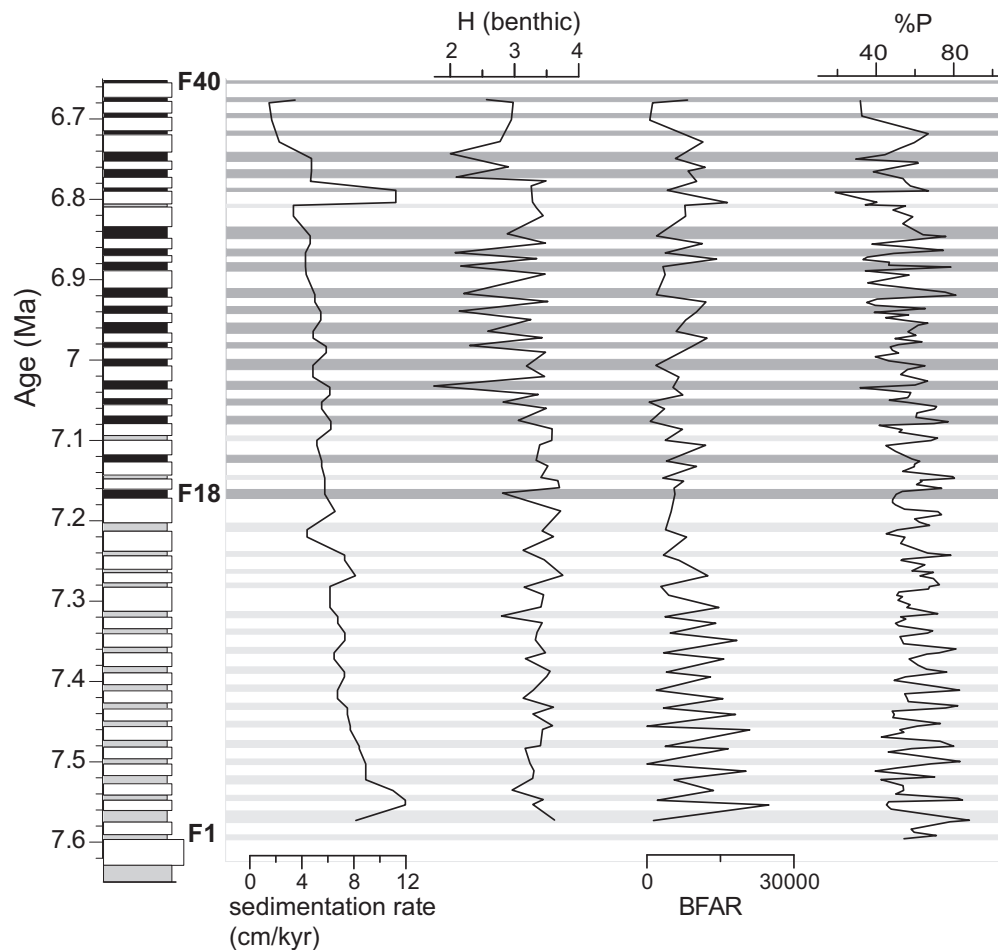


Fig. 6. From left to right: the sedimentation rate in cm/kyr, the benthic foraminifera diversity (Shannon index H), the accumulation rates of benthic foraminifera (BFAR, number of specimens/cm²/kyr) and the percentage of planktic foraminifera in the total counts of foraminiferal assemblages. Horizontal bars correspond to the schematic lithology: light grey for grey marls, darker grey for sapropelic layers, white for the light-coloured homogeneous marls.

4.1.1. Multivariate analysis

Multivariate analysis included hierarchical cluster analysis and principal components analysis (PCA). The dendrogram resulting from cluster analysis shows two main clusters I and II with a negative correlation of ± -0.15 (Fig. 7). Cluster I is divided at the zero level in sub-clusters 1a and 1b. Cluster 1a represents taxa decreasing in abundance in the sapropel of cycle F18 (7.17 Ma; Fig. 8). This counts especially for the taxa in subcluster 1a2. In addition, the maximum abundances of taxa in subcluster 1a1 shift from the grey marls to the light marls after 7.17 Ma (Fig. 8). Cluster 1b is composed of taxa present throughout the record. Until ~6.8 Ma this group of taxa shows maximum abundances in the light marls, with the exception of cycle F22 (Fig. 8). In the younger part of the section, maximum abundances of this group occur more randomly. Cluster II represents the taxa dominating after 7.17 Ma, especially in the sapropels at the levels where these are well developed (Fig. 8). The first three principal components axes (PC1–3) are considered and together explain 70% of the variance in the data (Fig. 7; PC1: 42.7%, PC2: 17%; PC3: 11.5%). The first axis (PC1) is loaded positively by species dominating in the sapropels and grey marls after 7.17 Ma (cycle F18; Fig. 9; Table 1). Dominantly loading (> 0.4 , Table 1) are *Bolivina dilatata/spathulata*, *Bulimina elongata* and *Uvigerina cylindrica gaudryinoides*; in addition, *Bolivina arta*, *B. tortuosa* and *B. striata* have positive loadings (> 0.2) on PC1. These taxa reach (much) higher abundances in the grey and sapropelic layers, especially or exclusively after cycle F18. Dominantly loading the first axis on the negative side (< -0.4) are *U. proboscidea* and *Trifarina bradyi*, which together with

other negatively loading taxa occur mainly in the light marls and disappear or decrease in abundance around cycle F18. The trend of PC1 follows the relative abundances of *B. dilatata/spathulata* and of species in Cluster II of the dendrogram (Fig. 6, 7). The most positively loading species (> 0.5 , Table 1) on PC2 is *Bolivina plicatella*, together with *B. dilatata/spathulata* (> 0.35). Most negatively loading is *U. cylindrica gaudryinoides* (< -0.6). Scores of PC2 show a distinct correlation with precession below cycle F18 (positive in light marls, negative in grey marls), and anti-correlation with the abundance data of *U. cylindrica gaudryinoides* between the cycles F22 and F32 (Fig. 9). *Bolivina plicatella* also loads positively on PC3 (> 0.7). Other taxa loading positively (> 0.3) are species in the group of epiphytes, among others *Discorbinella bertheloti*, *Discorbis* sp. 1, and *Ehrenbergina pacifica*. The axis is loaded negatively (< -0.4) by *B. aculeata*, *C. ungerianus*, *Lenticulina* spp. and *U. peregrina*, species of which the maximum abundances shift from grey marls to light marls after 7.17 Ma. Especially below cycle F18 the trend of PC3 covaries with the summed abundances of taxa with a potentially epiphytic life mode (Fig. 3, 7). The precessional cyclicity is clearly reflected.

4.2. Planktic foraminifera

The original data set of Calieri (1996) contains 30 taxa (species, species groups and genera). Species and species groups relevant to this study are shown in Fig. 10. *Globigerina bulloides*, *G. falconensis*, *Globigerinita glutinata* and *Turborotalita quinqueloba* are more abundant in the

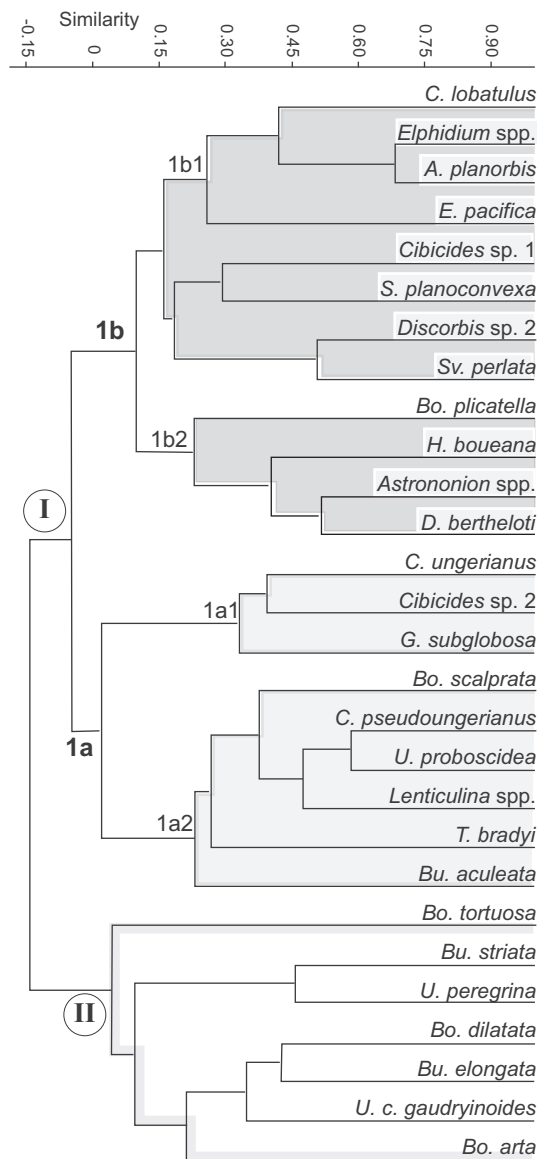


Fig. 7. Dendrogram resulting from R-mode hierarchical cluster analysis (UPGMA, correlation). Cluster I includes the potential epiphytes, the epifauna and the shallow infauna not tolerating stressed bottom-water environments. Cluster II includes shallow to deep infaunal species tolerating moderate to severe (oxygen) stress.

light marls, although the pattern in the younger part of the section is less clear. The *Globigerinoides* species, *Globigerinella siphonifera*, *Orbulina* spp. and the neogloboquadrinids are generally more abundant in the grey marls and the sapropels. Maximum abundances of the neogloboquadrinids occur in cycles F30–32, in F31 with one maximum in the light marl.

The diversity of the planktic foraminifera (Shannon-Wiener index; *H* (planktic) in Fig. 11) fluctuates between 1.5 and 2.5 and is generally higher in the grey marls and the sapropels. Larger fluctuations at the base of the section, before ~7.4 Ma (cycle F10) are followed by lower amplitude fluctuations until cycle F18 (7.17 Ma). Low diversity occurs in the light marl of cycle F22; after this minimum, the trend follows the abundance of the *Globigerinoides* group.

The numbers of planktic foraminifera per gram of dry sediment (PF/g) range between nearly zero and 2000 specimens per gram and are more irregular than the BFAR (see Fig. 6), but generally higher in the light-coloured marls (mean ~ 1500 specimens/g) than in the grey and

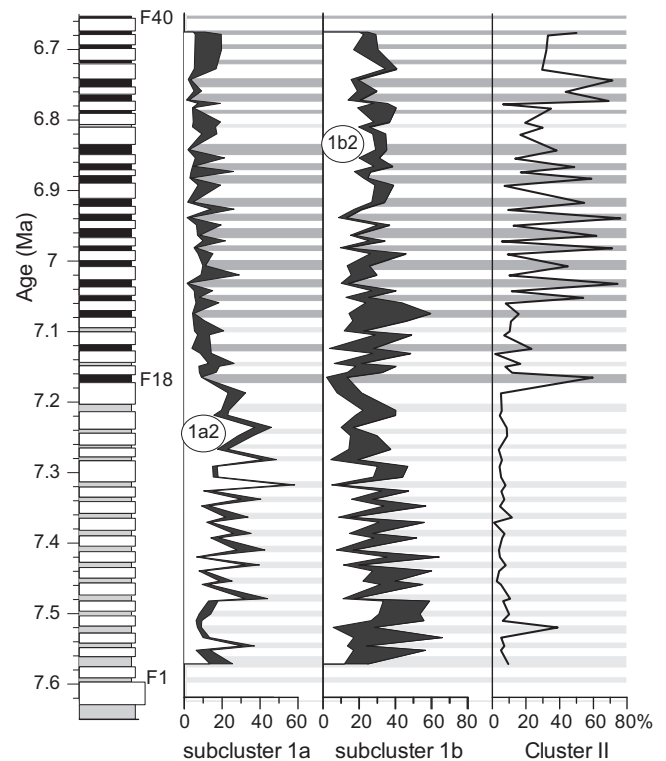


Fig. 8. Summed relative abundances of taxa in the (sub-) clusters of the dendrogram in Figure 7. Left panel: subcluster 1a of Cluster I with subdivision in smaller clusters 1a1 (in black) and 1a2 (in white). Middle panel: subcluster 1b of Cluster I with subdivision in smaller clusters 1b1 (in black) and 1b2 (in white). Right panel: Cluster II.

sapropelic layers (mean ~ 500 specimens/g). The PF/g are at a minimum in cycles F22–F25 (7.08–6.08 Ma). The patterns of the sea surface temperatures (SST) and the ratio between warm-oligotrophic and cold-eutrophic planktic foraminifera (WO/(WO + CE)) show the same characteristics, which is not surprising since there is much overlap in the species used to construct the curves.

Both the SST and the WO/(WO-CE) ratio range between 0.125 and 0.85 and are generally higher in the grey marls and sapropels (0.75) than in the light marls (~0.4). The regularly increasing trend from the base of the section upward is interrupted at cycle F20 with a minimum between cycles F22 and F24. Above cycle F24 the SST and the WO/(WO + CE) ratio show a similar variation as the *Globigerinoides* group.

5. Discussion

5.1. Palaeobathymetry

Previous reconstructions of the depositional depth in the lower part of the Faneromeni section range from outer neritic (Santarelli et al., 1998) to upper bathyal (300–400 m: Kouwenhoven et al., 2003; 400–550 m: Moissette et al., 2018). Moissette et al. (2018) reported shallowing-upwards to inner neritic depths in the upper part of the section. Depth reconstructions based on distributions of benthic foraminifera are often problematic, since many taxa have a large depth range. Several transfer functions based on benthic foraminifera have been developed and compared to improve the constraint on palaeodepths (e.g., Van der Zwaan et al., 1990; Hohenegger, 2005; Baldi and Hohenegger, 2008; Avnaim-Katav et al., 2015; Milker et al., 2017; Pérez-Asensio, 2021), but each method has limitations, the more so in sequences built of contrasting lithologies including homogeneous marls and sapropels. The reconstruction of palaeodepth in Kouwenhoven et al.

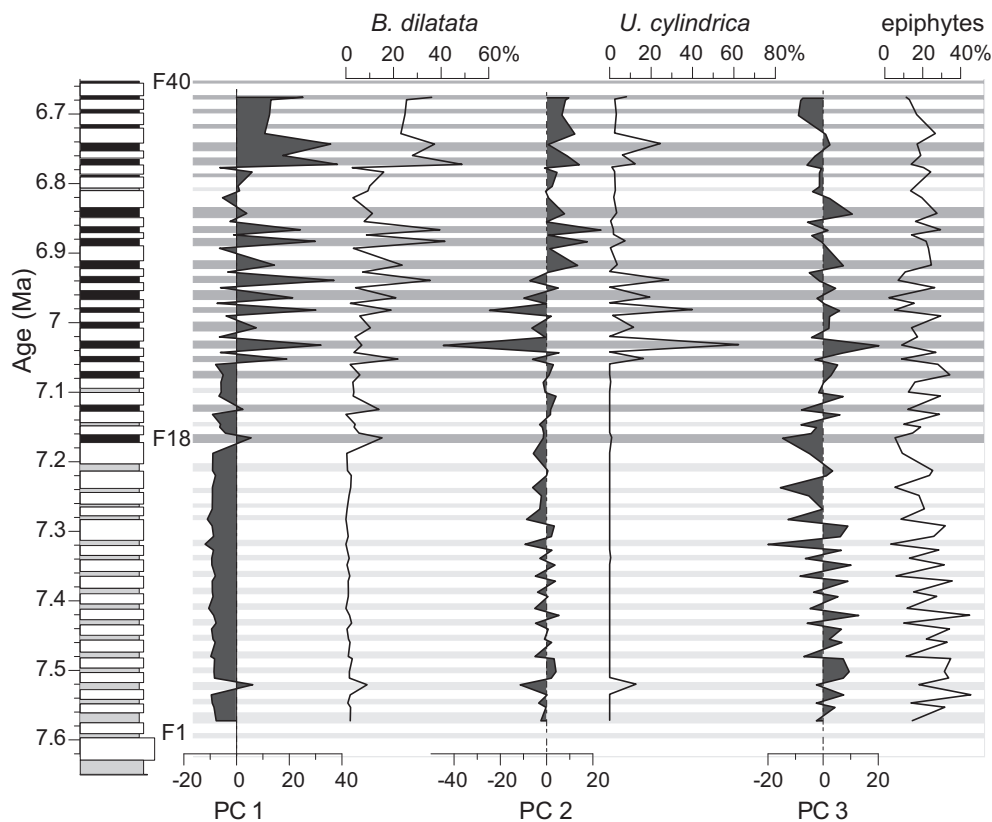


Fig. 9. The scores of the principal component axes 1–3 plotted next to the species or species groups with dominant loadings. For explanation see text.

Table 1

Species loadings on principal component axes 1–3.

Benthic taxon	PC 1	PC 2	PC 3
<i>Asterigerina planorbis</i>	−0.2675	0.0397	0.2939
<i>Astrononion</i> spp.	−0.2818	0.2465	0.1634
<i>Bolivina arta</i>	0.2704	0.2907	−0.0369
<i>Bolivina dilatata/spathulata</i>	0.9186	0.3568	−0.1586
<i>Bolivina plicatella</i>	−0.0902	0.5906	0.7049
<i>Bolivina scalprata miocenica</i>	−0.2145	−0.1854	−0.1384
<i>Bolivina tortuosa</i>	0.2272	0.0310	0.1471
<i>Bulimina aculeata</i>	−0.2693	−0.1381	−0.5839
<i>Bulimina elongata</i>	0.4440	0.0394	0.0091
<i>Bulimina striata</i>	0.2984	−0.2468	−0.2236
<i>Cibicides lobatulus</i>	−0.2181	−0.0428	0.1267
<i>Cibicides ungerianus</i>	−0.3205	−0.0056	−0.4780
<i>Cibicides</i> sp. 1	−0.3113	0.0471	0.1059
<i>Cibicides</i> sp. 2	−0.2698	0.0769	−0.0566
<i>Cibicidoides pseudoungerianus</i>	−0.2795	−0.2850	−0.3487
<i>Discorbinella bertheloti</i>	−0.2673	0.2266	0.3094
<i>Discorbis</i> sp. 1	−0.3454	0.1675	0.3206
<i>Ehrenbergina pacifica</i>	−0.3046	0.0586	0.3770
<i>Elphidium</i> spp.	−0.2998	0.1662	0.2652
<i>Globocassidulina subglobosa</i>	−0.2659	0.0731	−0.1860
<i>Hanzawaia boueana</i>	−0.0274	0.0261	0.2214
<i>Lenticulina</i> spp.	−0.3740	−0.3070	−0.4397
<i>Siphonina planoconvexa</i>	−0.3478	−0.0352	0.0340
<i>Svratkina perlata</i>	−0.2484	0.0649	0.1831
<i>Trifarina bradyi</i>	−0.4317	−0.0432	−0.0080
<i>Uvigerina cylindrica gaudryinoides</i>	0.7381	−0.6202	0.2472
<i>Uvigerina peregrina</i>	−0.0760	−0.0664	−0.4243
<i>Uvigerina proboscidea</i>	−0.4434	−0.1944	−0.1289

(2003) was based on planktic-benthic ratios of foraminifera (expressed as %P), and the transfer function in Van der Zwaan et al. (1990) because the relative percentage of planktic taxa increases with depth and distance to shore (Van der Zwaan et al., 1990 and references therein).

However, as Fig. 3 illustrates the %P fluctuates on a precessional scale throughout the period studied and is up to 40% higher in the grey marls and the sapropels, except in cycles F35 and F36. Using the transfer function of Van der Zwaan et al. (1990), these fluctuations in %P suggest palaeodepth changes between shelf and slope on a precessional scale, and consequently are unrealistic. More likely, these fluctuations are caused either by increased organic flux to the sea floor or lowered oxygen levels in the grey marls and sapropels, both potentially inducing a %P deviating from open marine, undisturbed conditions (e.g., Berger and Diester-Haass, 1988; Van der Zwaan et al., 1990; Van Hinsbergen et al., 2005; Jorissen et al., 2007; Dorst and Schönfeld, 2013).

Instead of transfer functions, here we were able to use groups of species with a limited depth range for an estimation of water depth. Most discorbids (e.g., *Discorbinella bertheloti*), *Bolivina plicatella*, several *Elphidium* species (e.g., *E. aculeatum*, *E. crispum*, *E. macellum*), *Rosalina* spp., and several taxa present in low abundances (e.g., *Gavelinopsis praegeri* (syn. *G. lobatulus*), *Glauvolutina* spp., *Planorbina mediterranea*, *Sigmoilopsis schlumbergeri*, *Spirillina vivipara*, and *Spiroplectinella* and *Textularia* spp.) are (potentially) epiphytes: they have been found living part, or all of their life span on algae and sea grasses or on their rhizomes. A number of these taxa occur on Pliocene and Recent *Posidonia* seagrass meadows (e.g., Langer, 1993; Ribes et al., 2000; Semeniuk, 2000; Semeniuk, 2001; Morigi et al., 2005; Moissette et al., 2007; Debenay and Payri, 2010; Mateu-Vicens et al., 2014; Mateu-Vicens et al., 2016). At present, *Posidonia* spp. occur in a depth range extending from inner shelf up to 40–50 m water depth, occasionally up to 80 m (e.g., Duarte, 1991). The epiphytic foraminifer taxa are present throughout the Faneromeni section with abundances of 30–40% in the light marls, whereas epifaunal/shallow infaunal taxa which normally occur more frequently in deeper, upper and middle bathyal environments such as *Cibicidoides bradyi*, *C. kullenbergi*, *C. pachyderma*, *Planulina ariminensis*, *Siphonina reticulata*, *Sphaeroidina bulloides* and *Uvigerina proboscidea* (Fig. 4a, b; Appendix A: e.g., Linke and Lutze, 1993; Altenbach et al.,

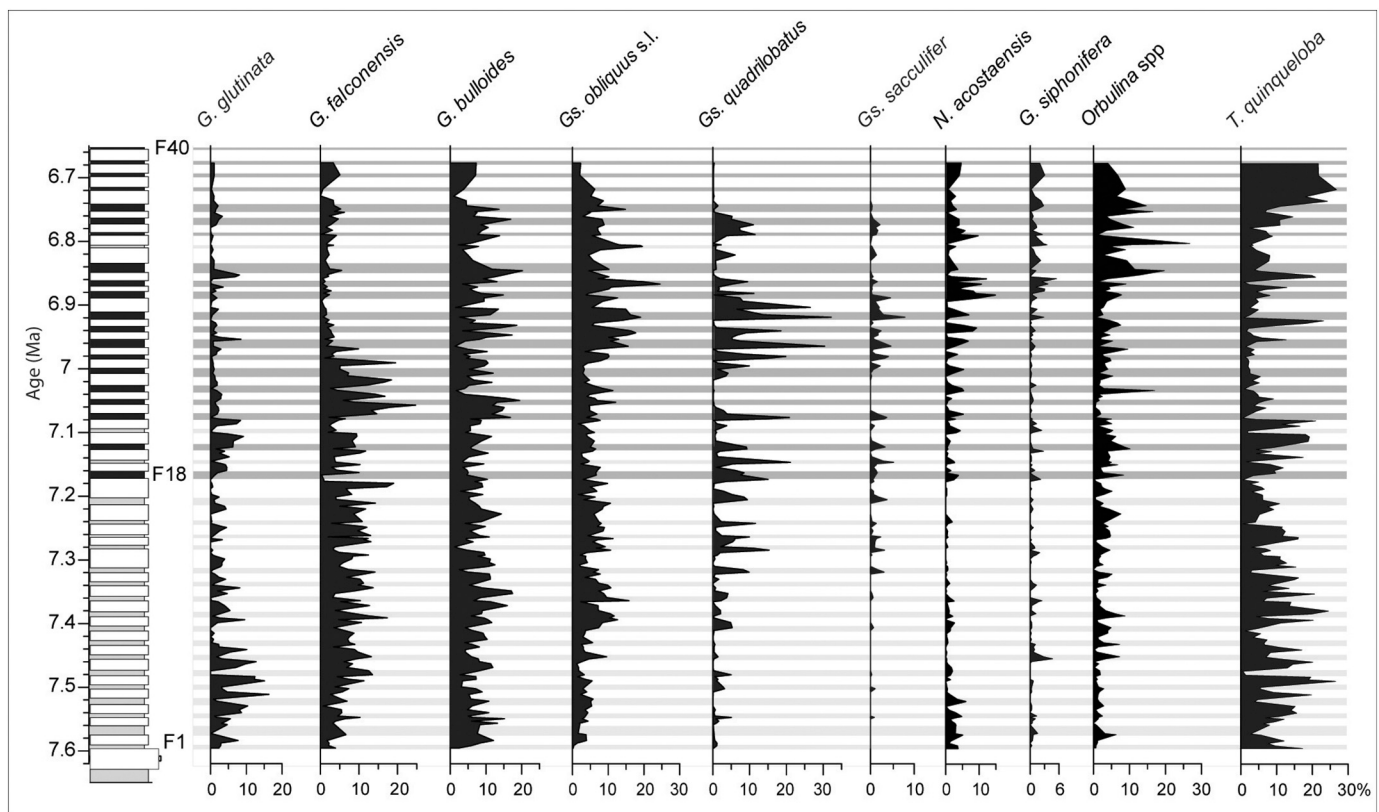


Fig. 10. Relative abundances of planktic foraminifera showing the correlation with precessional cyclicity. *Globigerina bulloides*, *G. falconensis*, *Globigerinita glutinata* and *Turborotalita quinqueloba* show higher abundances in the light marls. The *Globigerinoides* species, *Globigerinella siphonifera*, *Orbulina* spp. and *Neogloboquadrina acostaensis* show higher abundances in the grey marls and the sapropelic layers.

1999; Altenbach et al., 2003; De Rijk et al., 2000; Licari and Mackensen, 2005) occur in low abundances, generally below 5%. The %P in the grey and sapropelic layers is not considered representative. The %P in the light marls is ~40–45% in the larger part of the section. Gibson (1989), evaluating the ratio between planktic and benthic foraminifera from the north-eastern coast of the US, the western Pacific and the Gulf of Aqaba (Red Sea), found 50% of benthic foraminifera generally corresponding with a depth of 80–85 m. Schnitker (1971) found an abrupt increase of the abundance of planktic foraminifera (measured as specimens per cm³ of sediment) on the North Carolina shelf around 70 m, where *Globigerina bulloides* locally occurred in fairly high numbers in a water depth of 30 m. Abundances of planktic foraminifera further increased towards the shelf edge, but already around 70 m the assemblages were relatively diverse. In the Bay of Bengal Chowdhury et al. (2003) found 20–50% planktic foraminifera on the middle shelf (20–80 m), dominated by *Globigerinoides ruber* (similar ecological requirements as *Globigerinoides obliquus*, Kontakiotis et al., 2019 and references therein). *Globigerina bulloides* occurred on the inner shelf (~30 m). Wilson and Hayek (2019) reported the occurrence of 35 morphospecies of planktic foraminifera from 16 shelf stations (132–157 m) off northern Trinidad. This indicates that a relatively diverse planktic assemblage can already be found at middle- to outer shelf depths and suggests that the palaeodepth of the Faneromeni section during the period studied was probably corresponding to middle-outer shelf. The data neither confirm the continuous shallowing found by Moissette et al. (2018), or the bathyal palaeodepth reconstructed in the studies of these authors and Kouwenhoven et al. (2003) for the lower part of the section. The palaeodepth found in this study is in agreement with the depth reconstruction of Santarelli et al. (1998) which was based on high relative percentages of the outer neritic dinoflagellate cyst taxa *Spiniferites* and *Achmosphaera*.

5.2. Astronomically induced palaeoecological fluctuations

Astronomically induced palaeoecological signals are present in both benthic and planktic organisms and are generally coupled. The astronomical signals are used in benthic foraminiferal stable isotope records (e.g., Zachos et al., 2001; Lisiecki and Raymo, 2005), but less well documented in benthic foraminiferal assemblages. Below, we discuss astronomical (precessional) cyclicity in the Faneromeni section, for both surface and bottom-water organisms. We also anticipate on changes that were recorded in the benthic, but hardly in the pelagic realm: the change at 7.17 Ma (for more details we refer to section 5.3).

5.2.1. Surface waters

The short period shifts in the benthic and planktic foraminiferal abundances are associated with the lithological alternations (Fig. 4, 10), which in turn are related to precessional cyclicity. The relation between planktic foraminifera abundances and astronomical cyclicity has been so well established (overview in Hilgen et al., 2015) that abundance fluctuations of planktic species have been used to reconstruct cyclicity where visual lithological alternations are absent or not well developed (e.g., Sprovieri et al., 1996; Bulian et al., 2021).

In the Faneromeni section, the planktic foraminiferal diversity H (PF), the SST based on planktic foraminifera counts, and the warm-oligotrophic/cold eutrophic (WO/(WO + CE)) ratio are higher in the grey marls and the sapropels (Fig. 11). This implies that surface waters were warmer and more oligotrophic in the grey and sapropelic layers than in the light marls, in agreement with the higher abundances of subtropical taxa such as *Globigerinella siphonifera* and the *Globigerinoides* group (cf. Pérez-Folgado et al., 2003; Siero et al., 2003; Violanti et al., 2007). The detailed response of planktic foraminifera to seasonality and surface-water environments differs per species and species groups (e.g., Conan and Brummer, 2000; Jonkers and Kucera, 2015; Mallo et al.,

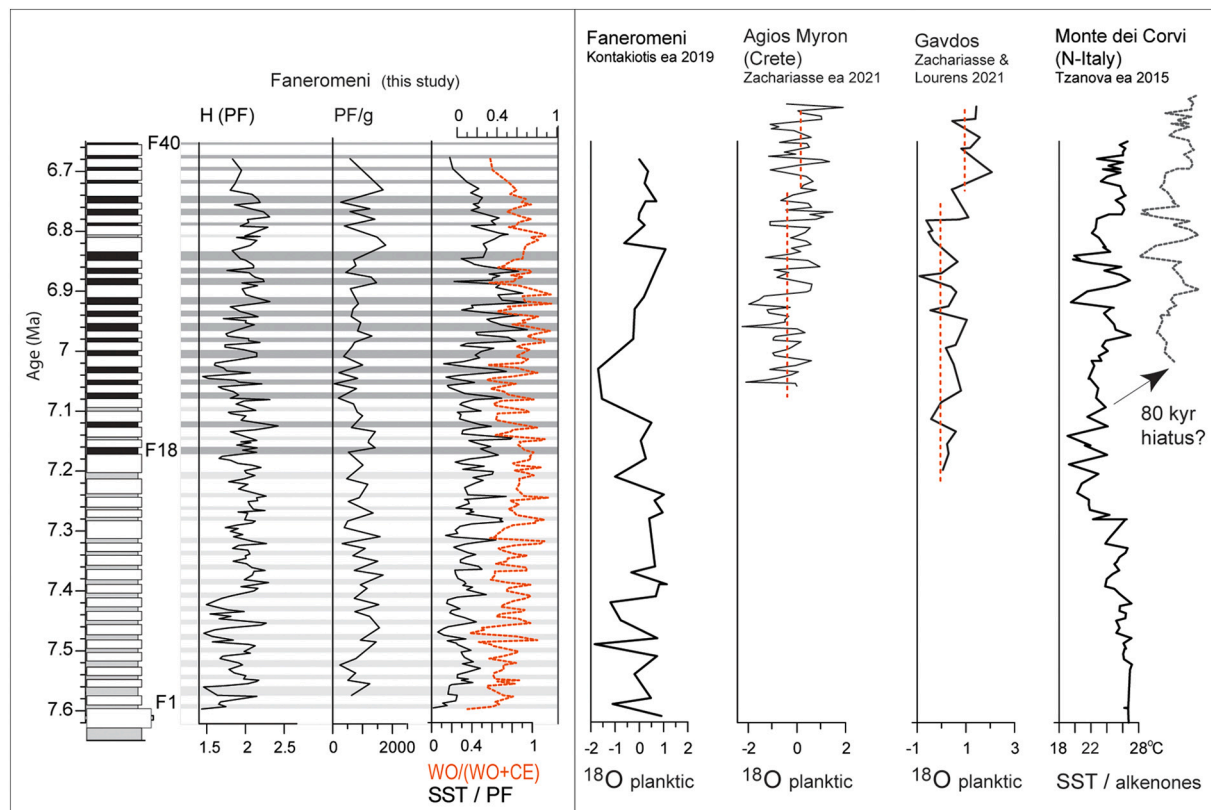


Fig. 11. The left panel shows data from this study. From left to right: H(PF) = the diversity of the planktic foraminifera; PF/g = the numbers of planktic foraminifera per gram of sediment; the SST/PF = the sea surface temperatures (SST) calculated from the planktic foraminifera and the WO/(WO + CE) ratio, the ratio between warm-oligotrophic and cold-eutrophic planktic species (for species included in the calculation of SST and WO/(WO + CE) see Methods section 3.2). The panels to the right show the oxygen isotopes measured on planktic foraminifera from the Faneromeni section (Kontakiotis et al., 2019), the Agios Myron sections on Crete (Zachariasse et al., 2021) and the Metochia section on Gavdos (Zachariasse and Lourens, 2021). To the very right the sea surface temperatures as reconstructed on basis of alkenone undersaturation rates in the Italian Monte dei Corvi section (Tzanova et al., 2015). For explanation see text.

2017; Rebotim et al., 2017), but temperature exerts a major influence on the distribution of planktic foraminifera. The symbiont-bearing planktic species seem less dependent on organic flux and more responsive to temperature limits (Jonkers and Kucera, 2015 and references therein). We have included in the warm and oligotrophic (WO) species group of the WO/(WO/CE) ratio the surface-dwelling, mostly symbiont-bearing (sub-) tropical species, such as *Globigerina siphonifera*, *Orbulina* spp., and most *Globigerinoides* spp. (e.g., Mallo et al., 2017; Jonkers and Kucera, 2015). Although the neogloboquadrinids were included in the ‘cold-eutrophic’ group by Sierro et al. (2003) and showed maximum abundances in the upper part of diatomites on Gavdos (Pérez-Folgado et al., 2003), they occur almost exclusively in the grey marls and sapropels in the Faneromeni section. Neogloboquadrinids are most abundant after winter mixing in eutrophic spring waters when thermal stratification builds up (Hemleben et al., 1989; Pujol and Vergnaud-Grazzini, 1995). The simultaneous presence of warm-oligotrophic, surface-dwelling and symbiont-bearing species and neogloboquadrinids (*N. acostaensis*) suggests that stratification of the water started spring and (early) summer, with a well-developed deep chlorophyll maximum (DCM) (e.g., Rohling et al., 2015 and references therein) concentrating the organic matter below an oligotrophic mixed layer. Negri and Villa (2000), studying calcareous nannofossils of the Faneromeni section, found lower abundances of calcareous nannofossils in the grey and sapropelic layers. The relative abundances of *Helicosphaera* and *Rhabdosphaera* spp. were higher and the abundances of small *Reticulofenestra* spp. were lower. Since small *Reticulofenestra* are interpreted as upwelling species, upwelling would not have prominent in the grey and sapropelic layers. *Helicosphaera carteri* was related to high temperatures and *Rhabdosphaera* to the presence of a DCM (Negri and Villa, 2000 and

references therein). This is in agreement with the planktic foraminifer data.

In contrast, the light-coloured, homogeneous marls are characterized by lower diversity (H), and lower WO/(WO + CE) ratios and SST, but also by higher planktic flux rates (specimens per gram of sediment: PF/g; Fig. 11). The light marls show higher abundances of species occurring in relatively cool and eutrophic waters (e.g., *Globigerina bulloides*; *G. falconensis*, *Turborotalita quinqueloba*, Fig. 10). Most of these species do not host symbionts (an exception is *Globigerinita glutinata*; e.g., Jonkers and Kucera, 2015). Winter mixing of the water column enhances the availability of organic matter in spring and favours species responding to organic flux. The higher abundances of *G. bulloides* and *T. quinqueloba* in the light marls suggest upwelling in spring and early summer. *Globigerina bulloides* is usually reported as a species responding with high relative abundances to cool, upwelling waters (e.g., Conan and Brummer, 2000; Sierro et al., 2003; Bárcena et al., 2004; Mallo et al., 2017; Wilson and Hayek, 2019; Darling et al., 2017). *Turborotalita quinqueloba* is also a species responding to upwelling, but not in numbers comparable to *G. bulloides*. This species probably tolerates deviating salinity (e.g., Kroon et al., 1988; Van de Poel, 1992). Monospecific assemblages consisting of *T. quinqueloba* were recorded around 6.7 Ma in Falconara (Sicily), in the Sorbas Basin (Spain) and Gavdos (Blanc-Valeron et al., 2002; Sierro et al., 2003; Zachariasse and Lourens, 2021) and have been interpreted as a signal for early salinity rise before the salinity crisis. This would be in agreement with Santarelli et al. (1998), who found salinity-tolerant dinocysts around 6.8 Ma in the Faneromeni section, although euryhaline species usually also tolerate low salinity. Negri and Villa (2000) found higher abundances of small placoliths (small-sized *Reticulofenestra* spp.) in the light marls, indicating

upwelling and high surface-water productivity, in agreement with the planktic foraminifer data.

5.2.2. Bottom waters

The benthic foraminifera indicate most favourable bottom-water conditions in the light marls. The BFAR have been used as a palaeo-productivity proxy, since higher foraminiferal accumulation rates have been reported to point towards higher nutrient fluxes (Herguera and Berger, 1991; Herguera, 1992). The BFAR are higher in the light marls, especially below cycle F18 where the abundances of deep infaunal stress markers are low. The ratio between epifaunal and infaunal species (E/I ratio) is consistently higher in the light marls. Higher abundances of the (potential) epiphytes are also found in the light marls (Fig. 6). Most epiphytes only tolerate low-oxygen conditions for a limited period, although attached species living in rhizomal microhabitats need to tolerate lower oxygen conditions overnight (but >2 mL/L; Langer, 1993). The light marls in the lower part of the section represent normal marine continental shelf settings, where the bottom-water oxygen content and the organic matter flux are usually high enough to support a diverse benthic assemblage and a well differentiated microhabitat distribution (e.g., De Stigter et al., 1988; Langezaal et al., 2006). This supports a generally well-mixed water column as indicated by the planktic assemblages. The grey marls reflect a more restricted environment with lower BFAR and lower abundance of the epiphytes and epifaunal species (Fig. 6), although below cycle F18 the diversity is comparable. Somewhat less favourable bottom-water conditions in the grey marls are in agreement with more prominent stratification of the water column, indicated by the planktic assemblages. However, the changes starting at 7.17 Ma in the benthic environment are not seen in the planktic assemblages and cannot be explained by changes in surface water productivity or stratification.

Starting in cycle F18 (7.17 Ma) the overall palaeoenvironmental conditions in the benthic environment worsened. The sapropelic layers above cycle F18 were deposited in a more hostile environment than the grey marls below cycle F18. At the same time, in the light marls the conditions appear to be less favourable than below cycle F18. The maximum abundances of several benthic taxa adapted to (mild) eutrophication and hypoxia shift from the grey marls below cycle F18 to the light marls above cycle F18 (e.g., *Bulimina aculeata*, *Cibicides ungerianus*; *Uvigerina peregrina*; Fig. 4). The benthic diversity (H; Fig. 6) shows larger shifts and is at minimum in the sapropels. After 7.17 Ma the infaunal benthic taxa *Bolivina dilatata/spatulata* and *Uvigerina cylindrica gaudryinoides* dominate the benthic assemblages in the sapropels (cluster II of the dendrogram; PC1 and PC2 (Fig. 4, 5, 8, 9). *Uvigerina cylindrica gaudryinoides* is considered stress-resistant, occurring in extremely eutrophic and hypoxic environments (Thomas, 1980; Van der Zwaan, 1982; Borsetti et al., 1986; Lutze, 1986). Dingle and Nelson (1993) and Schmiedl et al. (1997, as *Rectuvigerina cylindrica*) report the species (or a close relative) from Recent low-oxygen environments (< 2 mL/L) under elevated organic matter fluxes. In contrast, *B. dilatata/spatulata* was recently assigned in biomonitoring studies (Alve et al., 2016, as *Brizalina spatulata*; Jorissen et al., 2018, differentiating between *B. dilatata* and *B. spatulata*) to the group of species 'sensitive' to organic enrichment, i. e., occurring in oligo-mesotrophic, unpolluted environments and intolerant to excess organic input. *Bolivina dilatata/spatulata* was found in the core of the oxygen minimum zone (OMZ) in the Arabian Sea (Janink et al., 1998, as *B. spatulata*; Schumacher et al., 2007, as *Bolivina* aff. *B. dilatata*). In seasonality studies in the Bay of Biscay, Fontanier et al. (2003, as *B. spatulata*) and Langezaal et al. (2006, as *B. dilatata/spatulata*) found the taxon responding with rapid reproduction to seasonal (spring/early summer), pulsed supply of fresh phytodetritus in an otherwise oligotrophic environment.

Hypoxia during sapropel deposition has been ascribed to an increase of primary productivity, and/or increased preservation of organic matter caused by pre-existing bottom water anoxia (Rohling et al., 2015 and references therein). Decreasing deep-water ventilation due to warming

and water-mass stratification are alternative mechanisms driving hypoxia at the sea floor (e.g., Pälike et al., 2014). The extreme dominance of *Bolivina dilatata/spatulata* in sapropels especially after 6.90 Ma (cycles F26–31, and F35 and upward) suggests these sapropels were probably associated with decreasing oxygenation rather than with continuous eutrophication.

In our study the detailed development within a precessional cycle cannot be resolved but given that warm oligotrophic planktic taxa occurring in stratified waters still dominate in the sapropelic layers, it is likely that decreased deep-water ventilation, rather than high surface productivity caused the deposition of the sapropels (cf. Filippelli et al., 2003; Pérez-Folgado et al., 2003; Sierro et al., 2003), possibly caused by longer residence time of the deep waters. Differences probably exist between sapropels (e.g., Melki et al., 2010) and the sapropels dominated by *Uvigerina cylindrica gaudryinoides* may have been deposited under more continuous eutrophy.

It is noteworthy that the abundances of *B. dilatata/spatulata* and *U. cylindrica gaudryinoides* decrease in cycles F33 and F34 (6.81–6.79 Ma), just below the slumped level, where the grey marl of F33 is only weakly developed. Moreover, the Shannon-Wiener index remains high in this period. These features indicate a temporarily less stressed bottom-water environment associated with the 400-kyr eccentricity minimum around 6.80 Ma. Minor shifts also occur in the planktic foraminifer abundances and diversity. This suggests that the foraminifera, like the dinoflagellates (Santarelli et al., 1998), also reflect longer astronomical signals, but such a relation could not be substantiated in our data.

5.3. Long-term changes: stepwise severance of the Mediterranean-Atlantic connections

5.3.1. Restriction of bottom waters after 7.17 Ma (Faneromeni cycle F18)

The most prominent long-term shift in the abundances of benthic foraminiferal ecological groups in the Faneromeni section started in the first 'true' sapropel of cycle F18, which shows a temporary dominance of the shallow infaunal taxa *Bulimina striata* and *Uvigerina peregrina*, together with *Bolivina dilatata/spatulata* adding up to ~45% abundance. *Siphonina reticulata* and *Cibicides bradyi* were not recorded after 7.17 Ma and *C. kullenbergi*, *P. ariminensis* and *Siphonina planoconvexa* eventually disappeared too (Fig. 3a, b; Appendix A). The decline or disappearance of the relatively scarce, bathyal epifaunal and shallow infaunal taxa during, or shortly after cycle F18 was caused by the installation of increasingly hypoxic palaeoenvironments, since these species are sensitive to hypoxia and marks the start of the development towards the salinity crisis. The change in benthic foraminiferal assemblages around 7.17 Ma can be correlated throughout the Mediterranean and is most evident in assemblages from bathyal marine deposits (Italy, Sicily, Gavdos: e.g., Seidenkrantz et al., 2000; Kouwenhoven et al., 2003). Although in shallower sections this palaeoenvironmental change at 7.17 Ma seemed less well expressed (for instance, in sections on Crete and Cyprus: Kouwenhoven et al., 2003; Kouwenhoven et al., 2006) or absent (Moissette et al., 2018), it is definitely clear in the Faneromeni section, but best reflected in the sapropels.

In their semiquantitative study of marine flora and fauna from three Cretan sections among which the Faneromeni section, Moissette et al. (2018) found no indications for continuing restriction before 6.72 Ma. Kontakiotis et al. (2019) studying assemblage composition and shell geochemistry of planktic foraminifera from Faneromeni found a decrease in sea surface temperatures (SST) and sea surface salinity (SSS) starting at, or just after the Tortonian-Messinian boundary, with large fluctuations of SSS in the younger part of the section seemingly unrelated to astronomical cyclicity. The studies by Moissette et al. (2018) and Kontakiotis et al. (2019) have larger sampling intervals than our study, and for this reason may have overlooked some details of the cyclicity and the transition in the benthic foraminiferal assemblages at 7.17 Ma. In contrast, Santarelli et al. (1998) found a clear response to orbital parameters and a shift in the palynological associations of the

Faneromeni section at ~7.17 Ma, marked by a sharp increase in the amplitude of the short period variations in the Sporomorphs versus Dinocysts (S–D) index, associated with increasing influence of the obliquity signal. However, no permanent change in palynological assemblages was recorded at 7.17 Ma. Similarly, the planktic foraminifera in our study show no clear and permanent reflection of the change in benthic assemblages in cycle F18; more permanent changes in the planktic assemblages are seen after 7 Ma. This is consistent with recent studies of Kontakiotis et al. (2019) and Zachariasse et al. (2021), where among others planktic foraminifera were studied. Calcareous nannofossils seem not to have recorded a permanent change at 7.17 Ma either (Negri and Villa, 2000; Kouwenhoven et al., 2006).

Although *Bolivina dilatata/spatulata* and *Uvigerina cylindrica gaudryinoides* became the dominant species after 7.17 Ma, they present different trends. A maximum abundance (60%) of *U. cylindrica gaudryinoides* occurred in the sapropel of cycle F24 at 7.03 Ma, corresponding to low abundance of *B. dilatata/spatulata*. Subsequently, the relative abundance of *U. cylindrica gaudryinoides* declined gradually, whereas *B. dilatata/spatulata* became increasingly dominant in the sapropels. Minima of the planktic-benthic ratio (%P) and the Shannon-Wiener index (H) are associated with the peak abundance of *U. cylindrica gaudryinoides* and this level is also visible in the PC2 scores (Fig. 9). Dominance of *U. cylindrica gaudryinoides* was noticed earlier in relatively shallow Pliocene shelf sections in the Heraklion basin of central Crete (Jonkers, 1984), where peak abundances (50–60%) occurred in well-developed, relatively thick sapropels. This is in agreement with its occurrence in extremely hypoxic and eutrophic environments (see section 5.2). The species is either absent (e.g., the Metochia section on Gavdos; Seidenkrantz et al., 2000), or reaching only low abundances in deeper Miocene Mediterranean sections (e.g., Monte del Casino section in the northern Apennines, Kouwenhoven et al., 1999). Apparently, its occurrence was restricted to the shelf during this period. It is likely that *U. cylindrica gaudryinoides* thrives under more permanent stressed conditions than *B. dilatata/spatulata* (see also section 5.2).

Throughout the Mediterranean, the benthic foraminiferal event at 7.17 Ma correlates with sedimentological changes, for instance in the Sorbas and Nijar Basins (Spain) with the onset of the Abad marl Formation, a cyclic alternation of indurated white marls and softer, grey marls overlying calcarenites of the Azagador member (e.g., Sierro et al., 2001 and references therein). In the Faneromeni section, the precession minima (insolation maxima) are from cycle F18 upwards dominantly expressed as sapropelic layers, instead of grey marls. In many homogeneous-sapropel alternations throughout the Mediterranean the period after 7.17 Ma is characterized by the more regular occurrence of sapropels (e.g., Hilgen et al., 1995; Krijgsman et al., 1995; Seidenkrantz et al., 2000), suggesting increased sensitivity of the Mediterranean to changes in the hydrological budget (e.g., Sierro et al., 2003; Gladstone et al., 2007). This might also explain the relatively large shifts in $\delta^{13}\text{C}$ and $\delta^{18}\text{O}$ when compared to oceanic stable isotope records. The late Miocene (Tortonian through Messinian) global cooling, estimated at ~6 °C was recorded in both surface and deep waters (e.g., Zachos et al., 2001; Herbert et al., 2016; Holbourn et al., 2018). Moreover, a remarkable global decrease of carbon isotopes occurred during the latest Miocene (~7.60–6.60 Ma) dubbed the late Miocene carbon isotope shift (LMCIS). Both the late Miocene cooling found in open ocean SST and $\delta^{18}\text{O}$ records, and the LMCIS are reflected in Mediterranean records, where the amplitudes tend to be larger, with cooling in the order of 9–10 °C and a $\delta^{13}\text{C}$ drop of >1‰ (e.g., Sprovieri et al., 1996; Seidenkrantz et al., 2000; Hodell et al., 2001; Kouwenhoven et al., 2003; Tzanova et al., 2015; Kontakiotis et al., 2019; Bulian et al., 2022).

5.3.2. Surface- and deep-water environmental changes after 7.17 Ma and the second restriction phase around 6.8–6.7 Ma

For several benthic taxa, the association with lithology changes above cycle F18. The highest abundances of several species in cluster 1a of the dendrogram shift from grey marls to light marls after ~7.1 Ma

(Fig. 4, 8). This is most evident in *Cibicides ungerianus*, *Cibicides* sp. 2, *Gyroidina soldanii*, *Bulimina aculeata* and (in cluster II) *Uvigerina peregrina*. Especially the latter two taxa are considered relatively opportunistic, shallow infaunal taxa tolerating some hypoxia and relatively high organic flux (e.g., De Rijk et al., 2000). This implies that, above cycle F18, the environment during deposition of the light marls became more hostile, approximating the conditions in the grey marls below cycle F18. The BFARs continue to be higher in the light-coloured marls above cycle F18; however, the pattern should be interpreted with caution since, according to Naidu and Malmgren (1995), BFARs are not a reliable productivity proxy in low-oxygen environments.

The second restriction phase probably started around 6.8–6.7 Ma. *Bolivina dilatata/spatulata* plays an even more dominant role after 6.77 Ma (cycle F35; Fig. 4). It is not only abundant in the sapropels, but also shows a ~25% frequency in the light marls. *Uvigerina cylindrica gaudryinoides* re-occurs with 15–25% abundance in the sapropels of cycles F35 and F36 (6.78–6.74 Ma), together with *Bolivina dilatata/spatulata* adding up to nearly 70% of the benthic assemblage and the Shannon-Wiener diversity index drops to 2 (Fig. 4, 6). *Bolivina dilatata/spatulata* was mentioned as a taxon that might tolerate elevated salinity (Van der Zwaan, 1982; Drinia et al., 2007), although in studies on Recent foraminifera mainly the relation of *B. dilatata/spatulata* with low oxygen is stressed (see text section 5.2). *Uvigerina cylindrica gaudryinoides* is according to Thomas (1980) 'indifferent' to salinity changes. These taxa dominate the benthic assemblages at Faneromeni from cycle F35 (6.77 Ma) upwards.

Around the same time, the abundances of the planktic *Globigerinoides* spp., associated with oligotrophic surface waters, decline at this level (Fig. 10), and the frequency of the planktic foraminifer *Turborotalita quinqueloba* increases to 30% in cycle F36 (~6.74 Ma). This species is associated with cool surface waters and high surface productivity due to upwelling and/or vertical mixing of the water column (Sierro et al., 2003 and references therein). Together with relatively high abundances of *G. bulloides* this indicates eutrophic environments whereby *T. quinqueloba*, as an opportunistic taxon, can dominate over other species (Sierro et al., 2003). In addition, it was suggested that *T. quinqueloba* tolerates hypersaline surface waters (Kroon et al., 1988; Bijma et al., 1990; Van de Poel, 1992). Co-occurrence of *T. quinqueloba* with heavy oxygen isotope values was earlier noticed by Blanc-Valleron et al. (2002) in Sicilian sections.

The shift towards 0.7‰ heavier benthic $\delta^{18}\text{O}$, which was found around 6.74 Ma in the Agios Myron section (Crete), was explained in terms of a salinity increase of 2.9 ± 0.4 ppm in the bottom waters (Fig. 11; Zachariasse et al., 2021) since no indications for cooling were found. Temperature reconstructions based on alkenone undersaturation by Tzanova et al. (2015) do not show a temperature decrease. Tzanova et al. (op. cit.) suspected a ~80 kyr hiatus at 7.1 Ma, but this does not change these findings (Fig. 11). The decreasing SST in our study (Fig. 11) are more likely caused by increasing abundances of *Turborotalita quinqueloba* than with cooling. Zachariasse and Lourens (2021) found a similar and time-equivalent increase in the planktic and benthic $\delta^{18}\text{O}$ record in the Metochia section (Gavdos), coinciding with the start of intermittent occurrences of monospecific *T. quinqueloba* planktic faunas. In the dinoflagellate record of Santarelli et al. (1998) the second restriction phase is reported around 6.68 Ma (Faneromeni cycle F39) and is characterized by a lower S–D index (indicating less continental input) and low dinocyst species diversity. In the study by Santarelli et al. (1998 and references therein), the onset of hypersaline conditions in the surface waters is marked by the increasing dominance (up to 74%) of the dinocyst *Homotryblium tenuispinosum*, which was found to tolerate high salinity. Pross and Schmiedl (2002) also interpreted *H. tenuispinosum* as a high-salinity species in the Oligocene of the Rhine Graben. According to Dybkjaer (2004) who studied material from the Oligocene of Jylland, *Homotryblium* species are euryhaline. The planktic oxygen isotope record of Kontakiotis et al. (2019) shows a shift to heavier values after 7.1 Ma (Fig. 11), but this was not interpreted as a salinity rise. According to

Zachariasse and Lourens, 2021 the $\delta^{18}\text{O}$ and foraminifer data from Gavdos indicate that rising salinity affected surface and bottom waters around the same time, i.e., 6.74 ± 0.04 Ma. This age corresponds to cycle F36 of the Faneromeni section, where we see increasing abundance of *T. quinqueloba* and temporary, maximum abundances of *B. dilatata/spatulata* and *U. cylindrica gaudryinoides*. However, more data are needed to evaluate a possible salinity rise as early as 6.74 Ma.

6. Conclusions

Environmental changes affecting the Faneromeni section on Crete (Greece) between 7.57 and 6.67 Ma, the period preceding the Messinian salinity crisis (MSC) were reconstructed using foraminiferal assemblages. For this study, the previously published benthic foraminiferal record of the light marls (1 sample per cycle) was completed by adding the data from grey marls and sapropels resulting in a coverage of 2 samples per precessional cycle. The benthic foraminiferal data was re-evaluated together with selected planktic foraminiferal data.

The lithology consists of light-coloured marls alternating with grey marls before, and dominantly sapropels after cycle F18 (midpoint sapropel at 7.17 Ma) in a cyclic pattern that has been correlated to precession. The sedimentary sequence at Faneromeni was deposited at middle- to outer neritic (shelf) depth and no major shallowing or deepening was recorded during the time interval studied. Depth constraint is based on benthic and planktic assemblages, among others the continuous presence and proportion of potentially epiphytic taxa, of which several are living on seagrasses (such as *Posidonia* meadows), together with the low abundances of bathyal benthic taxa. Benthic foraminifera record the precessional cyclicity and the previously reported change in the marine bottom-water environment in cycle F18, around 7.17 Ma: the level where the first 'true' sapropel was deposited at Faneromeni. This benthic foraminiferal event can be correlated throughout the Mediterranean and is characterized by the disappearance of benthic species intolerant to hypoxia. The disappearance of these taxa is related to the more hostile conditions at the seafloor caused by a restriction phase of the Mediterranean-Atlantic gateways through northern Morocco and southern Spain. Planktic organisms did not clearly record this event at 7.17 Ma, but they were affected later during the Messinian. The high abundances of stress-tolerant species occurring from cycle F18 onwards in the sapropels, such as *Bolivina dilatata/spatulata*, indicate an oxygen-stressed environment; at the same time the light marls also became more hostile to benthic taxa. Comparing the benthic with the planktic foraminiferal distribution and the WO/(WO + CE) ratio, and in line with earlier publications it appears that hypoxia was more instrumental in the deposition of at least part of the sapropels than high surface-water productivity.

The bottom-water restriction at 7.17 Ma previously seemed less severe and less instantaneous at shallow-water sites such as Faneromeni, than at deeper water locations where the number of bathyal taxa was much higher and the event more distinct. However, when the sapropelic layers are considered, the expression of the 7.17 Ma event is as clear in Faneromeni as at deeper sites.

Just as in other Mediterranean sections the proxies indicate a second restriction step at Faneromeni around 6.8–6.7 Ma. Benthic and planktic foraminifera suggest more extreme environments, including a rise in salinity, although a salinity rise as early as ~6.8–6.7 Ma is still subject to discussion. In nearby sections on Crete and Gavdos a salinity rise appears to occur simultaneously in surface and bottom waters at 6.74 Ma. Just as the first restriction step at 7.17 Ma, this second step was probably associated with continuing restriction of the Mediterranean.

CRedit author statement

Jing Lyu: conceptualization, methodology, data acquisition (benthic foraminifera), writing - original draft preparation.

Tanja Kouwenhoven: conceptualization, methodology, data

acquisition (benthic foraminifera), supervision, writing - reviewing and editing.

Roberta Calieri: sample preparation, data acquisition (planktonic foraminifera).

Lucas Lourens: resources, supervision, writing - reviewing and editing, sample curation.

Declaration of Competing Interest

The authors declare that they have no known competing financial interests or personal relationships that could have appeared to influence the work reported in this paper.

Acknowledgements

Gerrit van 't Veld and Geert Ittmann[†] prepared the benthos samples. Ronald Harting is thanked for his help with picking benthos in the sapropel samples. Two anonymous referees and the Editor are thanked for critical reading and constructive comments. This research did not receive any specific grant from funding agencies in the public, commercial, or not-for-profit sectors.

Appendix A. Supplementary data

Supplementary data to this article can be found online at <https://doi.org/10.1016/j.marmicro.2022.102107>.

References

- Altenbach, A.V., Pflaumann, U., Schiebel, R., Thies, A., Timm, S., Trauth, M., 1999. Scaling percentages and distributional patterns of benthic Foraminifera with flux rates of organic carbon. *J. Foramin. Res.* 29, 173–185.
- Altenbach, A.V., Lutze, G.F., Schiebel, R., Schönfeld, J., 2003. Impact of interrelated and interdependent ecological controls on benthic foraminifera: an example from the Gulf of Guinea. *Palaeogeogr. Palaeoclimatol.* 197, 213–238. [https://doi.org/10.1016/S0031-0182\(03\)00463-2](https://doi.org/10.1016/S0031-0182(03)00463-2).
- Alve, E., Korsun, S., Schönfeld, J., Dijkstra, N., Golikova, E., Hess, S., Husum, K., Panieri, J., 2016. Foraminiferal: a sensitivity index based on benthic foraminiferal faunas from North-East Atlantic and Arctic fjords, continental shelves and slopes. *Mar. Micropaleontol.* 122, 1–12. <https://doi.org/10.1016/j.marmicro.2015.11.001>.
- Antonarakou, A., Drinia, H., Tsaparas, N., Dermizakis, M.D., 2007. Micropaleontological parameters as proxies of late Miocene surface water properties and paleoclimate in Gavdos Island, eastern Mediterranean. *Geodiversitas* 29, 379–399.
- Avnaim-Katav, S., Hyams-Kaphzan, O., Milker, Y., Almogi-Labin, A., 2015. Bathymetric zonation of modern shelf benthic foraminifera in the Levantine Basin, eastern Mediterranean Sea. *J. Sea Res.* 99, 97–106. <https://doi.org/10.1016/j.seares.2015.02.006>.
- Baldi, K., Hohenegger, J., 2008. Paleocology of benthic foraminifera of the Baden-Sooss section (Badenian, Middle Miocene, Vienna Basin, Austria). *Geol. Carpath.* 59, 411–424.
- Bárcena, M.A., Flores, J.A., Sierro, F.J., Pérez-Folgado, M., Fabres, J., Calafat, A., Canals, M., 2004. Planktonic response to main oceanographic changes in the Alboran Sea (Western Mediterranean) as documented in sediment traps and surface sediments. *Mar. Micropaleontol.* 53, 423–445. <https://doi.org/10.1016/j.marmicro.2004.09.009>.
- Berger, W.H., Diester-Haass, L., 1988. Paleoproductivity: The benthic/planktonic ratio in foraminifera as a productivity index. *Marine Geology* 81, 15–25.
- Bijma, J., Faber Jr., W.W., Hemleben, Ch., 1990. Temperature and salinity limits for growth and survival of some planktonic foraminifera in laboratory cultures. *J. Foramin. Res.* 20, 95–116.
- Blanc-Valleron, M.M., Pierre, C., Caulet, J.P., Caruso, A., Rouchy, J.M., Cespuoglio, G., Sprovieri, R., Pestrea, S., Di Stefano, E., 2002. Sedimentary, stable isotope and micropaleontological records of paleoceanographic change in the Messinian Tripoli Formation (Sicily, Italy). *Palaeogeogr. Palaeoclimatol.* 185, 255–286.
- Borsetti, A.M., Iaccarino, S., Jorissen, F.J., Poignant, A., Sztrakos, K., van der Zwaan, G. J., Verhallen, P.J.J.M., 1986. The Neogene development of *Uvigerina* in the Mediterranean, in: *Atlantic-European Oligocene to Recent Uvigerina*, edited by: van der Zwaan, G. J., Jorissen, F. J., Verhallen, P. J. J. M., and von Daniels, C. H., *Utrecht Micropaleontological Bulletin*, 35, Utrecht, The Netherlands, pp. 183–228.
- Bulian, F., Sierro, F.J., Ledesma, S., Jiménez-Espejo, F.J., Bassetti, M.A., 2021. Messinian West Alboran Sea record in the proximity of Gibraltar: Early signs of Atlantic-Mediterranean gateway restriction. *Mar. Geol.* 434, 106430. <https://doi.org/10.1016/j.margeo.2021.106430>.
- Bulian, F., Kouwenhoven, T.J., Jiménez-Espejo, F.J., Andersen, N., Krijgsman, W., Sierro, F.J., 2022. Impact of the Messinian global cooling and Mediterranean-Atlantic connectivity on deep-sea communities in the Westernmost Mediterranean

- Sea. *Palaeogeogr. Palaeoclimatol.* 589. <https://doi.org/10.1016/j.palaeo.2022.110841> article 110841.
- Calieri, R., 1996. Planktonic foraminiferal biostratigraphy and cyclostratigraphy of the Tortonian-Messinian boundary: preliminary results from the Faneromeni section (Crete). *Palaeogeogr. Palaeoclimatol.* 6, 329–338.
- Capella, W., Hernández-Molina, F.J., Flecker, R., Hilgen, F.J., Hsain, M., Kouwenhoven, T.J., van Oorschot, M., Sierro, F.J., Stow, D.A.V., Trabuco-Alexandre, J., Tullbure, M.A., de Weger, W., Yousfi, M.Z., Krijgsman, W., 2017. Sandy contourite drift in the late Miocene Rifian Corridor (Morocco): Reconstruction of depositional environments in a foreland-basin seaway. *Sediment. Geol.* 355, 31–57. <https://doi.org/10.1016/j.sedgeo.2017.04.004>.
- Capella, W., Barhoun, N., Flecker, R., Hilgen, F.J., Kouwenhoven, T.J., Matenco, L.C., Sierro, F.J., Tullbure, M.A., Yousfi, M.Z., Krijgsman, W., 2018. Palaeogeographic evolution of the late Miocene Rifian Corridor (Morocco): reconstructions from surface and subsurface data. *Earth Sci. Rev.* 180, 37–59. <https://doi.org/10.1016/j.earscirev.2018.02.017>.
- Capella, W., Flecker, R., Hernández-Molina, F.J., Simon, D., Meijer, P.Th., Rogerson, M., Sierro, F.J., Krijgsman, W., 2019. Mediterranean isolation preconditioning the Earth System for late Miocene climate cooling. *Nat. Sci. Rep.* 9, 3795. <https://doi.org/10.1038/s41598-019-40208-2>.
- Cerling, T.E., Harris, J.M., MacFadden, B.J., Leakey, M.G., Quade, J., Eisenmann, V., Ehleringer, J.R., 1997. Global Vegetation Change through the Miocene/Pliocene Boundary. *Nature* 389, 153–158.
- Chowdhury, K.R., Mahfuzul Haque, Md., Nasreen, N., Rashedul Hasan, Md., 2003. Distribution of planktonic foraminifera in the northern Bay of Bengal. *Sediment. Geol.* 155, 393–405.
- Conan, S.M.-H., Brummer, G.J.A., 2000. Fluxes of planktic foraminifera in response to monsoonal upwelling on the Somalia Basin margin. *Deep-Sea Res. II* (47), 2207–2227.
- Corbí, H., Soria, J.M., Giannetti, A., Yébenes, A., 2020. The step-by-step restriction of the Mediterranean (start, amplification, and consolidation phases) preceding the Messinian Salinity Crisis (climax phase) in the Bajo Segura basin. *Geo-Mar. Lett.* 40, 341–361. <https://doi.org/10.1007/s00367-020-00647-7>.
- Darling, K.F., Wade, C.M., Siccha, M., Trommer, G., Schulz, H., Abdolalipour, S., Kurasawa, A., 2017. Genetic diversity and ecology of the planktonic foraminifera *Globigerina bulloides*, *Turborotalita quinqueloba* and *Neoglobobulimina* pachyderma off the Oman margin during the late SW Monsoon. *Mar. Micropaleontol.* 137, 64–77.
- De Rijk, S., Jorissen, F.J., Rohling, E.J., Troelstra, S.R., 2000. Organic flux control on bathymetric zonation of Mediterranean benthic foraminifera. *Mar. Micropaleontol.* 40, 151–166.
- De Stigter, H.C., Jorissen, F.J., van der Zwaan, G.J., 1988. Bathymetric distribution and microhabitat partitioning of live (Rose Bengal stained) benthic Foraminifera along a shelf to bathyal transect in the southern Adriatic Sea. *J. Foramin. Res.* 28, 40–65.
- Debenay, J.P., Payri, C.E., 2010. Epiphytic foraminiferal assemblages on macroalgae in reefal environments of New Caledonia. *J. Foramin. Res.* 40, 36–60.
- Dingle, R.V., Nelson, G., 1993. Sea-bottom temperature, salinity and dissolved oxygen on the continental margin off south-western Africa. *S. Afr. J. Mar. Sci.* 13, 33–49. ISSN: 0257–7615.
- Dorst, S., Schönfeld, J., 2013. Diversity of benthic foraminifera on the shelf and slope of the NE Atlantic: Analysis of datasets. *J. Foramin. Res.* 43, 238–254.
- Drinia, H., Antonarakou, A., Tzapas, N., Kontakiotis, G., 2007. Palaeoenvironmental conditions preceding the Messinian Salinity Crisis: A case study from Gavdos Island. *Geobios* 40, 251–265. <https://doi.org/10.1016/j.geobios.2007.02.003>.
- Duarte, C.M., 1991. Seagrass depth limits. *Aquat. Bot.* 40, 363–377.
- Dybkaer, K., 2004. Dinocyst stratigraphy and palynofacies studies used for refining a sequence stratigraphic model—uppermost Oligocene to lower Miocene, Jylland, Denmark. *Review of Palaeobotany and Palynology* 131, 3–4.
- Farrell, J.W., Raffi, I., Janecek, T.R., Murray, D.W., Levitan, M., Dadey, K.A., Emeis, K.C., Lyle, M., Flores, J.A., Hovan, S., 1995. Late Neogene sedimentation patterns in the eastern equatorial Pacific Ocean, in: *Proceedings of the Ocean Drilling Program, Scientific Results*, 138, edited by: Pisias, N. G., Mayer, L. A., Janecek, T. R., Palmer-Julson, A., and van Andel, T. H., College Station, Texas, pp. 717–756. <https://doi.org/10.2973/odp.proc.sr.138.143.1995>.
- Filippelli, G.M., Sierro, F.J., Flores, J.A., Vázquez, A., Utrilla, R., Pérez-Folgado, M., Latimer, J.C., 2003. A sediment–nutrient–oxygen feedback responsible for productivity variations in late Miocene sapropel sequences of the western Mediterranean. *Palaeogeogr. Palaeoclimatol.* 190, 335–348.
- Flecker, R., Krijgsman, W., Capella, W., de Castro Martins, C., Dmitrieva, E., Mayser, J.P., Marzocchi, A., Modestou, S., Ochoa, D., Simon, D., Tullbure, M.A., van den Berg, B., van der Schee, M., de Lange, G., Ellam, R., Govers, R., Gutjahr, M., Hilgen, F., Kouwenhoven, T., Lofi, J., Meijer, P., Sierro, F.J., Bachiri, N., Barhoun, N., Alami, A. C., Chacon, B., Flores, J.A., Gregory, J., Howard, J., Lunt, D., Ochoa, M., Pancost, R., Vincent, S., Yousfi, M.Z., 2015. Evolution of the Late Miocene Mediterranean–Atlantic gateways and their impact on regional and global environmental change. *Earth Sci. Rev.* 150, 365–392. <https://doi.org/10.1016/j.earscirev.2015.08.007>.
- Flores, J.A., Sierro, F.J., Philippelli, G.M., Ángeles, B.M., Pérez-Folgado, M., Vázquez, A., Utrilla, R., 2005. Surface water dynamics and phytoplankton communities during deposition of cyclic late Messinian sapropel sequences in the western Mediterranean. *Mar. Micropaleontol.* 56, 50–79. <https://doi.org/10.1016/j.marmicro.2005.04.002>.
- Fontanier, C., Jorissen, F.J., Chaillou, G., David, C., Anschutz, P., Lafon, V., 2003. Seasonal and interannual variability of benthic foraminiferal faunas at 550 m depth in the Bay of Biscay. *Deep-Sea Res. Pt. I* (50), 457–494. [https://doi.org/10.1016/S0967-0637\(02\)00167-X](https://doi.org/10.1016/S0967-0637(02)00167-X).
- Gibson, T.G., 1989. Planktonic benthonic foraminiferal ratios: modern patterns and tertiary applicability. *Mar. Micropaleontol.* 15, 29–52.
- Gladstone, R., Flecker, R., Valdes, P., Lunt, D., Markwick, P., 2007. The Mediterranean hydrologic budget from a Late Miocene global climate simulation. *Palaeogeogr. Palaeoclimatol.* 251, 254–267. <https://doi.org/10.1016/j.palaeo.2007.03.050>.
- Hammer, Ø., Harper, D.A.T., Ryan, P., 2001. D.: Paleontological statistics software package for education and data analysis. *Palaeontol. Electron.* 4 (1), 9 pp. http://palaeo-electronica.org/2001_1/past/issue1_01.htm.
- Hemleben, C., Spindler, M., Anderson, O.R., 1989. *Modern Planktonic Foraminifera*. Springer, New York, pp. 1–363.
- Herbert, T.D., Lawrence, K.T., Tzanova, A., Peterson, L.C., Caballero-Gill, R., Kelly, C.S., 2016. Late Miocene global cooling and the rise of modern ecosystems. *Nat. Geosci.* 9, 843–847. <https://doi.org/10.1038/NGEO2813>.
- Herguera, J.C., 1992. Deep-sea benthic foraminifera and biogenic opal: glacial to postglacial productivity changes in the western equatorial Pacific. *Mar. Micropaleontol.* 19, 79–98.
- Herguera, J.C., Berger, W.H., 1991. Paleoproductivity from benthic foraminifera abundance: glacial to postglacial change in the west-equatorial Pacific. *Geology* 19, 1173–1176.
- Hilgen, F.J., Krijgsman, W., Langereis, C.G., Lourens, L.J., Santarelli, A., Zachariasse, W. J., 1995. Extending the astronomical (polarity) time scale into the Miocene. *Earth Planet. Sc. Lett.* 136, 495–510.
- Hilgen, F.J., Bissoli, L., Iaccarino, S., Krijgsman, W., Meijer, R., Negri, A., Villa, G., 2000. Integrated stratigraphy and astrochronology of the Messinian GSSP at Oued Akrech (Atlantic Morocco). *Earth Planet. Sc. Lett.* 182, 237–251.
- Hilgen, F.J., Kuiper, K.F., Krijgsman, W., Snel, E., van der Laan, E., 2007. Astronomical tuning as the basis for high resolution chronostratigraphy: the intricate history of the Messinian Salinity Crisis. *Stratigraphy* 4, 231–238.
- Hilgen, F. J., Lourens, L. J., and Van Dam, J. A., with contributions by Beu, A. G., Boyes, A. F., Cooper, R. A., Krijgsman, W., Ogg, J. G., Piller, W. E., and Wilson, D. S., The neogene period, in: *The Geologic Time Scale 2012*, edited by: Gradstein, F. M., Ogg, J. G., Schmitz, M. & Ogg, G., DOI: <https://doi.org/10.1016/B978-0-444-59425-9.00029-9>, 2012.
- Hilgen, F.J., Hinnov, L.A., Abdul Aziz, H., Abels, H.A., Batenburg, S., Bosmans, J.H., de Boer, B., Hüsing, S.K., Kuiper, K.F., Lourens, L.J., Rivera, T., Tuenter, E., van de Wal, R.S.W., Wotzlaw, J.F., Zeeden, C., 2015. Stratigraphic continuity and fragmentary sedimentation: the success of cyclostratigraphy as part of integrated stratigraphy, in: *Strata and Time: Probing the Gaps in Our Understanding*, edited by: Smith, D. G., Bailey, R. J., Burgess, P.M. & Fraser, A. J. Geological Society, London. Special Publications, 404, 157–197.
- Hixon, M.A., Brostoff, W.N., 1983. Damselfish as keystone species in reverse: intermediate disturbance and diversity of reef algae. *Science* 220, 511–513.
- Hodell, D.A., Benson, R.H., Kent, D.V., Boersma, A., Rakic-El Bied, K., 1994. Magnetostratigraphic, biostratigraphic, and stable isotope stratigraphy of an Upper Miocene drill core from the Salé Briqueterie (northwestern Morocco): a high-resolution chronology for the Messinian stage. *Paleoceanography* 9, 835–855.
- Hodell, D.A., Curtis, J.H., Sierro, F.J., Raymo, M.E., 2001. Correlation of late Miocene to early Pliocene sequences between the Mediterranean and North Atlantic. *Paleoceanography* 16, 164–178, 1999PA000487.
- Hohenegger, J., 2005. Estimation of environmental paleogradient values based on presence/absence data: a case study using benthic foraminifera for paleodepth estimation. *Palaeogeogr. Palaeoclimatol.* 217, 115–130. <https://doi.org/10.1016/j.palaeo.2004.11.020>.
- Holbourn, A.E., Kuhnt, W., Clemens, S.C., Kochhann, K.G.D., Jöhnck, J., Lübbert, J., Andersen, N., 2018. Late Miocene climate cooling and intensification of southeast Asian winter monsoon. *Nat. Commun.* 9, 1–13. <https://doi.org/10.1038/s41467-018-03950-1>.
- Hsu, K.J., Ryan, W.B.F., Cita, M.B., 1973. Late Miocene desiccation of the Mediterranean. *Nature* 242, 240–244.
- Jannink, N.T., Zachariasse, W.J., van der Zwaan, G.J., 1998. Living (Rose Bengal stained) benthic foraminifera from the Pakistan continental margin (northern Arabian Sea). *Deep-Sea Res. Pt. I* (45), 1483–1513.
- Jolivet, L., Augier, R., Robin, C., Suc, J.P., Rouchy, J.M., 2006. Lithospheric-scale geodynamic context of the Messinian Salinity Crisis. *Sediment. Geol.* 188, 9–33. <https://doi.org/10.1016/j.sedgeo.2006.02.004>.
- Jonkers, H.A., 1984. Pliocene benthonic foraminifera from homogeneous and laminated marls on Crete, Utrecht Micropaleontological Bulletins, 31, edited by: Drooger, C. W. Utrecht University, Utrecht, The Netherlands, 179 pp.
- Jonkers, L., Kucera, M., 2015. Global analysis of seasonality in the shell flux of extant planktonic Foraminifera. *Biogeosciences* 12, 2207–2226. <https://doi.org/10.5194/bg-12-2207-2015>.
- Jorissen, F.J., Fontanier, C., Thomas, E., 2007. Paleoceanographical proxies based on deep-sea benthic foraminiferal assemblage characteristics. In: *Proxies in Late Cenozoic Paleoceanography*, Pt. 2: Biological tracers and biomarkers, edited by: Hillaire-Marcel, C. and de Vernal, A. Elsevier, pp. 263–326.
- Jorissen, F.J., Nardelli, M.P., Almogi-Labin, A., Barras, C., Bergamin, L., Bicchì, E., El Kateb, A., Ferraro, L., McGann, M., Morigi, C., Romano, E., Sabbatini, A., Schweizer, M., Spezzaferri, S., 2018. Developing Foraminifera-AMBI for biomonitoring in the Mediterranean: species assignments to ecological categories. *Mar. Micropaleontol.* 140, 33–45. <https://doi.org/10.1016/j.marmicro.2017.12.006>.
- Keigwin, L.D., Shackleton, N.J., 1980. Uppermost Miocene carbon isotope stratigraphy of a piston core in the equatorial Pacific. *Nature* 284, 613–614.
- Kontakiotis, G., Besiou, E., Antonarakou, A., Zarkogiannis, S.D., Kostis, A., Mortyn, P.G., Moissette, P., Cornée, J.J., Schulbert, C., Drinia, H., Anastakis, G., Karakitsios, V., 2019. Decoding Sea surface and palaeoclimate conditions in the eastern

- Mediterranean over the Tortonian-Messinian transition. *Palaeogeogr. Palaeoclimatol.* 534, 109312 <https://doi.org/10.1016/j.palaeo.2019.109312>.
- Kouwenhoven, T.J., Seidnkrantz, M.-S., van der Zwaan, G.J., 1999. Deep-water changes: the near-synchronous disappearance of a group of benthic foraminifera from the late Miocene Mediterranean. *Palaeogeogr. Palaeoclimatol.* 152, 259–281.
- Kouwenhoven, T.J., Hilgen, F.J., van der Zwaan, G.J., 2003. Late Tortonian-early Messinian stepwise disruption of the Mediterranean-Atlantic connections: constraints from benthic foraminiferal and geochemical data. *Palaeogeogr. Palaeoclimatol.* 198, 303–319. [https://doi.org/10.1016/S0031-0182\(03\)00472-3](https://doi.org/10.1016/S0031-0182(03)00472-3).
- Kouwenhoven, T.J., Morigi, C., Negri, A., Giunta, S., Krijgsman, W., Rouchy, J.M., 2006. Paleoenvironmental evolution of the eastern Mediterranean during the Messinian: Constraints from integrated microfossil data of the Pissouri Basin (Cyprus). *Mar. Micropaleontol.* 60, 17–44. <https://doi.org/10.1016/j.marmicro.2006.02.005>.
- Krijgsman, W., Hilgen, F.J., Langereis, C.G., Zachariasse, W.J., 1994. The age of the Tortonian/Messinian boundary. *Earth Planet. Sci. Lett.* 121, 533.
- Krijgsman, W., Hilgen, F.J., Langereis, C.G., Santarelli, A., Zachariasse, W.J., 1995. Late Miocene magnetostratigraphy, biostratigraphy and cyclostratigraphy in the Mediterranean. *Earth Planet. Sci. Lett.* 136, 475.
- Krijgsman, W., Langereis, C.G., Zachariasse, W.J., Bocalletti, M., Moratti, G., Gelati, R., Iaccarino, S., Papani, G., Villa, G., 1999. Late Neogene evolution of the Taza-Quercif Basin (Rifian Corridor, Morocco) and implications for the Messinian salinity crisis. *Mar. Geol.* 153, 147–160.
- Krijgsman, W., Capella, W., Simon, D., Hilgen, F.J., Kouwenhoven, T.J., Meijer, P.Th., Sierro, F.J., Tulpure, M.A., van den Berg, B.C.J., van der Scher, M., Flecker, R., 2018. The Gibraltar corridor: watergate of the messinian salinity crisis. *Mar. Geol.* 403, 238–246. <https://doi.org/10.1016/j.margeo.2018.06.008>.
- Krijgsman, W., Palcu, D.V., Andreotto, F., Stoica, M., Mandic, O., 2020. Changing seas in the late Miocene Northern Aegean: a Paratethyan approach to Mediterranean basin evolution. *Earth Sci. Rev.* 210, 103386 <https://doi.org/10.1016/j.earscirev.2020.103386>.
- Kroon, D., Wouters, P.F., Moodley, L., Ganssen, G., Troelstra, S.R., 1988. Phenotypic variation of *Turborotalita quinqueloba* (Natland) tests in living populations and in the Pleistocene of an eastern Mediterranean piston core. In: *Planktonic Foraminifera as Tracers of Ocean-Climate History*, edited by: Brummer, G. J. A. and Kroon, D. Free University Press, Amsterdam, pp. 131–147.
- Kuiper, K.F., Hilgen, F.J., Steenbrink, J., Wijbrans, J.R., 2004. $^{40}\text{Ar}/^{39}\text{Ar}$ ages of tephras intercalated in astronomically tuned Neogene sedimentary sequences in the eastern Mediterranean. *Earth Planet. Sci. Lett.* 222, 583–597.
- Langer, M.R., 1993. Epiphytic foraminifera. *Mar. Micropaleontol.* 20, 235–265.
- Langereis, C.G., Zachariasse, W.J., Zijdeveld, J.D.A., 1984. Late Miocene magnetobiostratigraphy of Crete. *Mar. Micropaleontol.* 8, 261–281.
- Langezaal, A.M., Jorissen, F.J., Braun, B., Chaillou, G., Fontanier, C., Anschutz, P., van der Zwaan, G.J., 2006. The Influence of seasonal processes on geochemical profiles and foraminiferal assemblages on the outer shelf of the Bay of Biscay. *Cont. Shelf Res.* 26 <https://doi.org/10.1016/j.csr.2006.05.0051730-1755>.
- Laskar, J., 1990. The chaotic motion of the solar system: a numerical estimate of the size of the chaotic zones. *Icarus* 88, 266–291.
- Laskar, J., Joutel, F., Boudin, F., 1993. Orbital, precessional, and insolation quantities for the earth from -20 Myr to +10 Myr. *Astron. Astrophys.* 270, 522.
- Licari, L., Mackensen, A., 2005. Benthic foraminifera off West Africa (1°N to 32°S): do live assemblages from the topmost sediment reliably record environmental variability? *Mar. Micropaleontol.* 55, 205–233. <https://doi.org/10.1016/j.marmicro.2005.03.001>.
- Linke, P., Lutze, G.F., 1993. Microhabitat preferences of benthic foraminifera – a static concept or a dynamic adaptation to optimize food acquisition? *Mar. Micropaleontol.* 20, 215–234.
- Lisiecki, L.E., Raymo, M.E., 2005. A Pliocene-Pleistocene stack of 57 globally distributed benthic $\delta^{18}\text{O}$ records. *Paleoceanography* 20. <https://doi.org/10.1029/2004PA001071>.
- Lutze, G.F., 1986. *Uvigerina* species of the eastern North Atlantic. In: *Atlantic-European Oligocene to Recent Uvigerina*, edited by: van der Zwaan, G. J., Jorissen, F. J., Verhallen, P. J. J. M., and von Daniels, C. H., Utrecht Micropaleontological Bulletin, 35, Utrecht, The Netherlands, pp. 21–46.
- Mallo, M., Ziveri, P., Graham Mortyn, P., Schiebel, R., Grellaud, M., 2017. Low planktic foraminiferal diversity and abundance observed in a spring 2013 west-east Mediterranean Sea plankton tow transect. *Biogeosciences* 14, 2245–2266. <https://doi.org/10.5194/bg-14-2245-2017>.
- Manzi, V., Gennari, R., Hilgen, F., Krijgsman, W., Lugli, S., Roveri, M., Sierro, F.J., 2013. Age refinement of the Messinian salinity crisis onset in the Mediterranean. *Terra Nova* 25, 315–322. <https://doi.org/10.1111/ter.12038>.
- Manzi, V., Gennari, R., Lugli, S., Persico, D., Roveri, M., Gvrtzman, Z., 2021. Synchronous onset of the Messinian salinity crisis and diachronous evaporite deposition: New evidences from the deep Eastern Mediterranean basin. *Palaeogeogr. Palaeoclimatol.* 584. <https://doi.org/10.1016/j.palaeo.2021.110685>. Article 110685.
- Martha, S.O., Zulauf, G., Dörr, W., Binck, J.J., Nowara, P.M., Xypolias, P., 2018. The tectonometamorphic evolution of the Uppermost Unit south of the Dikti Mountains, Crete. *Geol. Mag.* 156, 1003–1026. <https://doi.org/10.1017/S0016756818000328>.
- Martin, J.M., Puga-Bernabéu, A., Aguirre, J., Braga, J.C., 2014. Miocene Atlantic-Mediterranean Seaways in the Betic Cordillera (Southern Spain), *Revista de la Sociedad Geológica de España*, 27, 175–186, ISSN (Internet): 2255–1379.
- Mateu-Vicens, G., Khokhlova, A., Sebastián-Pastor, T., 2014. Epiphytic foraminiferal indices as bioindicators in Mediterranean seagrass meadows. *J. Foramin. Res.* 44, 325–339.
- Mateu-Vicens, G., Sebastián, T., Khokhlova, A., Del Mar Leza, M., Deudero, S., 2016. Characterization of nitrogen and carbon stable isotopes in epiphytic foraminiferal morphotypes. *J. Foramin. Res.* 46, 271–284.
- Melki, T., Kallel, N., Fontugne, M., 2010. The nature of transitions from dry to wet conditions during sapropel events in the Eastern Mediterranean Sea. *Palaeogeogr. Palaeoclimatol.* 291, 267–285. <https://doi.org/10.1016/j.palaeo.2010.02.039>.
- Miller, Y., Weinkauff, M.F.G., Titschack, J., Freiwald, A., Krueger, S., Jorissen, F.J., Schmiedl, G., 2017. Testing the applicability of a benthic foraminiferal-based transfer function for the reconstruction of paleowater depth changes in Rhodes (Greece) during the early Pleistocene. *PLoS One* 12, e0188447. <https://doi.org/10.1371/journal.pone.0188447>.
- Moissette, P., Koskeridou, E., Cornée, J.J., François, G., Christophe, L., 2007. Spectacular preservation of seagrasses and seagrass-associated communities from the Pliocene of Rhodes, Greece. *Palaios* 22, 200–211. <https://doi.org/10.2110/palo.2005.p05-141r>.
- Moissette, P., Cornée, J.J., Antonarakou, A., Kontakiotis, G., Drinia, H., Koskeridou, E., Tsourou, T., Agiadi, K., Karakitsios, V., 2018. Paleoenvironmental changes at the Tortonian/Messinian boundary: a deep-sea sedimentary record of the eastern Mediterranean Sea. *Palaeogeogr. Palaeoclimatol.* 505, 217–233. <https://doi.org/10.1016/j.palaeo.2018.05.046>.
- Morigi, C., Jorissen, F.J., Fraticelli, S., Horton, B.P., Principi, M., Sabbatini, A., Capotondi, L., Curzi, P.V., Negri, A., 2005. Benthic foraminiferal evidence for the formation of the Holocene mud-belt and bathymetrical evolution in the Central Adriatic Sea. *Mar. Micropaleontol.* 57, 25–49. <https://doi.org/10.1016/j.marmicro.2005.06.001>.
- Naidu, P.D., Malmgren, B.A., 1995. Do benthic foraminifer records represent a productivity index in oxygen minimum zone areas? An evaluation from the Oman Margin, Arabian Sea. *Mar. Micropaleontol.* 26, 49–55.
- Negri, A., Villa, J., 2000. Calcareous nannofossil biostratigraphy, biochronology and palaeoecology at the Tortonian/Messinian boundary of the Faneromeni section (Crete). *Palaeogeogr. Palaeoclimatol.* 156, 195–209.
- Nijenhuis, I.A., Schenau, S.J., Van der Weijden, C.H., Hilgen, F.J., Lourens, L.J., Zachariasse, W.J., 1996. On the origin of upper Miocene sapropelites: A case study from the Faneromeni section, Crete (Greece). *Paleoceanography* 11, 633–645, 96PA01963.
- Pälike, C., Delaney, M.L., Zachos, J.C., 2014. Deep-sea redox across the Paleocene-Eocene thermal maximum. *Geochim. Geophys. Geosyst.* 15, 1038–1053. <https://doi.org/10.1002/2013GC005074>.
- Pérez-Asensio, J.N., 2021. Quantitative palaeobathymetric reconstructions based on foraminiferal proxies: a case study from the Neogene of south-West Spain. *Palaeontology* 64, 475–488. <https://doi.org/10.1111/pala.12538>.
- Pérez-Asensio, J.N., Aguirre, J., Schmiedl, G., Civis, J., 2012. Messinian paleoenvironmental evolution in the lower Guadalquivir Basin (SW Spain) based on benthic foraminifera. *Palaeogeogr. Palaeoclimatol.* 326–328, 135–151. <https://doi.org/10.1016/j.palaeo.2012.02.014>.
- Pérez-Asensio, J.N., Aguirre, J., Schmiedl, G., Civis, J., 2014. Messinian productivity changes in the northeastern Atlantic and their relationship to the closure of the Atlantic-Mediterranean gateway: implications for Neogene palaeoclimate and paleoceanography. *J. Geol. Soc.* 171, 389–400. <https://doi.org/10.1144/jgs2013-032>.
- Pérez-Folgado, M., Sierro, F.J., Bárcena, M.A., Flores, J.A., Vázquez, A., Utrilla, R., Hilgen, F.J., Krijgsman, W., Filippelli, G.M., 2003. Western versus eastern Mediterranean paleoceanographic response to astronomical forcing: a high-resolution microplankton study of precession-controlled sedimentary cycles during the Messinian. *Palaeogeogr. Palaeoclimatol.* 190, 317–334.
- Phillips, D., Matchan, E.L., Honda, M., Kuiper, K.F., 2017. Astronomical calibration of $^{40}\text{Ar}/^{39}\text{Ar}$ reference minerals using high-precision, multi-collector (ARGUSVI) mass spectrometry. *Geochim. Cosmochim. Acta* 196, 351–369. <https://doi.org/10.1016/j.gca.2016.09.027>.
- Pross, J., Schmiedl, G., 2002. Early Oligocene dinoflagellate cysts from the Upper Rhine Graben (SW Germany): paleoenvironmental and paleoclimatic implications. *Mar. Micropaleontol.* 45, 1–24.
- Pujol, C., Vergnaud-Grazzini, C., 1995. Distribution patterns of live planktic foraminifera as related to regional hydrography and productive systems of the Mediterranean Sea. *Mar. Micropaleontol.* 25, 187–217.
- Rebotim, A., Voelker, A.H.L., Jonkers, L., Wanek, J.J., Meggers, H., Schiebel, R., Fraile, I., Schulz, M., and Kucera, M., 2017. Factors controlling the depth habitat of planktonic foraminifera in the subtropical eastern North Atlantic. *Biogeosciences* 14, 827–859. <https://doi.org/10.5194/bg-14-827-2017>.
- Ribes, T., Salvadó, H., Romero, J., Del Pilar Gracia, M., 2000. Foraminiferal colonization on artificial seagrass leaves. *J. Foramin. Res.* 30, 192–201.
- Rivera, T.A., Storey, M., Zeeden, C., Hilgen, F.J., Kuiper, K.F., 2011. A refined astronomically calibrated $^{40}\text{Ar}/^{39}\text{Ar}$ age for Fish Canyon sandine. *Earth Planet. Sci. Lett.* 311, 420–426. <https://doi.org/10.1016/j.epsl.2011.09.017>.
- Rohling, E.J., Marino, G., Grant, K.M., 2015. Mediterranean climate and oceanography, and the periodic development of anoxic events (sapropels). *Earth Sci. Rev.* 143, 62–97. <https://doi.org/10.1016/j.earscirev.2015.01.008>.
- Roveri, M., Flecker, R., Krijgsman, W., Lofi, J., Lugli, S., Manzi, V., Sierro, F.J., Bertini, A., Camerlenghi, A., de Lange, G.J., Govers, R., Hilgen, F.J., Hübscher, C., Meijer, P., Stoica, M., 2014. The Messinian Salinity Crisis: past and future of a great challenge for marine sciences. *Mar. Geol.* 352, 25–58. <https://doi.org/10.1016/j.margeo.2014.02.002>.
- Santarelli, A., Brinkhuis, H., Hilgen, F.J., Lourens, L.J., Versteegh, G.J.M., Visscher, H., 1998. Orbital signatures in a late Miocene dinoflagellate record from Crete (Greece). *Mar. Micropaleontol.* 33, 297–295.
- Schmiedl, G., Mackensen, A., Müller, P.J., 1997. Recent benthic foraminifera from the eastern South Atlantic Ocean: Dependence on food supply and water masses. *Mar. Micropaleontol.* 32, 249–287.
- Schnitker, D., 1971. Distribution of foraminifera on the North Carolina continental shelf. *Tulane Studies Geol. Paleontol.* 8 (4), 169–215.

- Schumacher, S., Jorissen, F.J., Dissard, D., Larkin, K.E., Gooday, A.J., 2007. Live (rose Bengal stained) and dead benthic foraminifera from the oxygen minimum zone of the Pakistan continental margin (Arabian Sea). *Mar. Micropaleontol.* 62, 45–73. <https://doi.org/10.1016/j.marmicro.2006.07.004>.
- Seidenkrantz, M.S., Kouwenhoven, T.J., Jorissen, F.J., Shackleton, N.J., van der Zwaan, G.J., 2000. Benthic foraminifera as indicators of changing Mediterranean–Atlantic water exchange in the late Miocene. *Mar. Geol.* 163, 387–407.
- Semeniuk, T.A., 2000. Spatial variability in epiphytic foraminifera from micro- to regional scale. *J. Foramin. Res.* 30, 99–109.
- Semeniuk, T.A., 2001. Epiphytic foraminifera along a climatic gradient, Western Australia. *J. Foramin. Res.* 31, 191–200.
- Shackleton, N.J., 1977. Carbon-13 in *UVIGERINA*: Tropical rainforest history and the equatorial Pacific carbonate dissolution cycles. In: *The Fate of Fossil Fuel CO₂ in the Oceans*, edited by: Anderson, N. R. and Malahoff, A. Springer, New York, pp. 401–427.
- Sierro, F.J., Hilgen, F.J., Krijgsman, W., Flores, J.A., 2001. The Abad composite (SE Spain): a Messinian reference section for the Mediterranean and the APTS. *Palaeogeogr. Palaeoclimatol.* 168, 141–169.
- Sierro, F.J., Flores, J.A., Francés, G., Vázquez, A., Utrilla, R., Zamarreño, I., Erlenkeuser, H., Bárcena, M.A., 2003. Orbitally-controlled oscillations in planktic communities and cyclic changes in western Mediterranean hydrography during the Messinian. *Palaeogeogr. Palaeoclimatol.* 190, 289–316.
- Sprovieri, R., Di Stefano, E., Sprovieri, M., 1996. High resolution chronology for late Miocene Mediterranean stratigraphic events. *Riv. Ital. Paleontol. S.* 102, 77–104.
- Thomas, E., 1980. Details of *Uvigerina* development in the Cretan Mio-Pliocene. *Utrecht Micropaleontological Bulletin*, 23, edited by: Drooger, C. W. Utrecht University, Utrecht, The Netherlands, 160 pp.
- Tulbure, M.A., Capella, W., Barhoun, N., Flores, J.A., Hilgen, F.J., Krijgsman, W., Kouwenhoven, T.J., Sierro, F.J., Yousfi, M.Z., 2017. Age refinement and basin evolution of the North Rifian Corridor (Morocco): no evidence for a marine connection during the Messinian Salinity Crisis. *Palaeogeogr. Palaeoclimatol.* 485, 416–432. <https://doi.org/10.1016/j.palaeo.2017.06.031>.
- Tzanova, A., Herbert, T.D., Peterson, L., 2015. Cooling Mediterranean Sea surface temperatures during the late Miocene provide a climate context for evolutionary transitions in Africa and Eurasia. *Earth Planet. Sc. Lett.* 419, 71–80. <https://doi.org/10.1016/j.epsl.2015.03.016>.
- Van Couvering, J.A., Castradori, D., Cita, M.B., Hilgen, F.J., Rio, D., 2000. The base of the Zanclean Stage and of the Pliocene Series. *Episodes* 23, 179–186.
- Van de Poel, H.M., 1992. Foraminiferal biostratigraphy and palaeoenvironments of the Miocene-Pliocene Carboneras-Nijar Basin (SE Spain). *Scr. Geol.* 102, 1–32.
- Van der Scher, M., van den Berg, B.C.J., Capella, W., Simon, D., Sierro, F.J., Krijgsman, W., 2018. New age constraints on the western Betic intramontane basins: a late Tortonian closure of the Guadalquivir Corridor? *Terra Nova*. <https://doi.org/10.1111/ter.12347>.
- Van der Zwaan, G.J., 1982. *Paleoecology of late Miocene Mediterranean foraminifera*, Utrecht Micropaleontological Bulletin, 25, edited by: Drooger, C. W. Utrecht University, Utrecht, The Netherlands, 201 pp.
- Van der Zwaan, G.J., Jorissen, F.J., de Stigter, H.C., 1990. The depth dependency of planktonic/benthic foraminiferal ratios: Constraints and applications. *Mar. Geol.* 95, 1–16.
- Van Hinsbergen, D.J.J., Meulenkamp, J.E., 2006. Neogene supra-detachment basin development on Crete (Greece) during exhumation of the South Aegean core complex. *Basin Res.* 18, 103–124. <https://doi.org/10.1111/j.1365-2117.2005.00282.x>.
- Van Hinsbergen, D.J.J., Kouwenhoven, T.J., van der Zwaan, G.J., 2005. Palaeobathymetry in the backstripping procedure: correction for oxygenation effects on depth estimates. *Palaeogeogr. Palaeoclimatol.* 221, 245–265. <https://doi.org/10.1016/j.palaeo.2005.02.013>.
- Verhallen, P.J.J.M., 1991. Late Pliocene to early Pleistocene Mediterranean mud-dwelling foraminifera; Influence of a changing environment on community structure and evolution. *Utrecht Micropaleontological Bulletin*, 40, edited by: Drooger, C. W. and van der Zwaan, G. J. Utrecht University, Utrecht, The Netherlands, 219 pp.
- Vincent, E., Killingley, J.S., Berger, W.H., 1980. The magnetic epoch 6 carbon shift: a change in the ocean's ¹³C/¹²C ratio 6.2 million years ago. *Mar. Micropaleontol.* 5, 185–203.
- Violanti, D., Mariano Gallo, L., Rizzi, A., 2007. Foraminiferal assemblages of the Bric della Muda laminites (Nizza Monferrato, Piedmont): Proxies of cyclic palaeoenvironmental changes in the early Messinian of Northwestern Italy. *Geobios* 40, 281–290. <https://doi.org/10.1016/j.geobios.2006.11.003>.
- Wilson, B., Hayek, L.-A.C., 2019. Planktonic foraminifera as indicators of oceanographic complexity on the southern Caribbean Sea continental shelf, Estuarine, Coastal and Shelf Science 228. Article 106359. <https://doi.org/10.1016/j.ecss.2019.106359>.
- Zachariasse, W.J., Lourens, L.J., 2021. The Messinian on Gavdos (Greece) and the status of currently used ages for the onset of the MSC and gypsum precipitation. *News. Stratigr.* <https://doi.org/10.1127/nos/2021/0677>.
- Zachariasse, W.J., van Hinsbergen, D.J.J., Fortuin, A.R., 2008. Mass wasting and uplift on Crete and Karpathos during the early Pliocene related to initiation of south Aegean left-lateral, strike-slip tectonics. *Geol. Soc. Am. Bull.* 120, 976–993. ISSN: 0016-7606.
- Zachariasse, W.J., van Hinsbergen, D.J.J., Fortuin, A.R., 2011. Formation and fragmentation of a late Miocene supradetachment basin in Central Crete: implications for exhumation mechanisms of high-pressure rocks in the Aegean forearc. *Basin Res.* 23, 678–701. <https://doi.org/10.1111/j.1365-2117.2011.00507.x>.
- Zachariasse, W.J., Kontakiotis, G., Lourens, L.J., Antonarakou, A., 2021. The Messinian of Agios Myron (Crete, Greece): a key to better understanding of diatomite formation on Gavdos (south of Crete). *Palaeogeogr. Palaeoclimatol.* 581 <https://doi.org/10.1016/j.palaeo.2021.110633>.
- Zachos, J., Pagani, M., Sloan, L., Thomas, E., Billups, K., 2001. Trends, rhythms, and aberrations in global climate 65 Ma to present. *Science* 292, 686–693.